

Relaxation in a Fuzzy Dark Matter Halo

BEN BAR-OR,¹ JEAN-BAPTISTE FOUVRY,^{1,*} AND SCOTT TREMAINE¹

¹*Institute for Advanced Study, Princeton, NJ 08540, USA*

ABSTRACT

Dark matter may be composed of light bosons, $m_b \sim 10^{-22}$ eV, with a de Broglie wavelength $\lambda \sim 1$ kpc in typical galactic potentials. Such “fuzzy” dark matter (FDM) behaves like cold dark matter (CDM) on much larger scales than the de Broglie wavelength, but may resolve some of the challenges faced by CDM in explaining the properties of galaxies on small scales ($\lesssim 10$ kpc). Because of its wave nature, FDM exhibits stochastic density fluctuations on the scale of the de Broglie wavelength that never damp. The gravitational field from these fluctuations scatters stars and black holes, causing their orbits to diffuse through phase space. We show that this relaxation process can be analyzed quantitatively with the same tools used to analyze classical two-body relaxation in an N -body system, and can be described by treating the FDM fluctuations as quasiparticles, with effective mass $\sim 10^7 M_\odot (1 \text{ kpc}/r)^2 (10^{-22} \text{ eV}/m_b)^3$ in a galaxy with a constant circular speed of 200 km s^{-1} . This novel relaxation mechanism may stall the inspiral of supermassive black holes or globular clusters due to dynamical friction at radii of a few hundred parsecs, and can heat and expand the central regions of galaxies. These processes can be used to constrain the mass of the light bosons that might comprise FDM.

1. INTRODUCTION

Despite the remarkable success of cosmological models based on cold dark matter (CDM) in explaining large-scale structure and other cosmological phenomena, CDM has faced challenges in predicting aspects of small-scale structure, such as the abundance of dwarf galaxies and the dark-matter density near the centers of galaxies (e.g., Weinberg et al. 2015). The solution to these problems may lie either in baryonic physics (e.g., feedback to the interstellar medium from supernovae or black holes) or in the properties of the dark matter itself.

In this paper, we examine aspects of the behavior of fuzzy dark matter (FDM), which is composed of bosons with extremely small masses, typically $m_b \sim 10^{-21}$ – 10^{-22} eV (e.g., Hu et al. 2000; Hui et al. 2017). The corresponding de Broglie wavelength at velocity v is $\lambda = h/(m_b v) \simeq 1.20 \text{ kpc} (10^{-22} \text{ eV}/m_b)(100 \text{ km s}^{-1}/v)$; on scales much larger than this, FDM behaves like CDM, but on small scales, it exhibits quite different properties and may match the observations better than CDM (e.g., Hui et al. 2017).

Several studies have argued that the mass range $m_b \lesssim$ a few $\times 10^{-21}$ eV is ruled out by constraints from the Lyman- α forest power spectrum (Viel et al. 2013; Armengaud et al. 2017; Iršič et al. 2017; Kobayashi et al. 2017; Nori et al. 2019), which would imply that FDM is indistinguishable from CDM in its effects on observed small-scale structure. However, (i) these constraints usually rely on assumptions (e.g., uniform ionizing background) that are plausible but may be oversimplified, (ii) the mass constraint can be much weaker in variants of the FDM model (e.g., Leong et al. 2018), and (iii) the dynamical processes discussed here can be important whether or not the FDM particle mass is small enough to influence small-scale structure.

Since FDM particles are bosons, density fluctuations in the dark matter are correlated over a distance of the order of the de Broglie wavelength. Hui et al. (2017) argued that the fluctuating gravitational force from an FDM field of mean density ρ is similar to that of a classical N -body system composed of quasiparticles with effective mass $m_{\text{eff}} \sim \rho \lambda^3$.

The relaxation time of a test particle orbiting in a stellar system of radius R , containing N bodies of mass m , is (Binney & Tremaine 2008)

$$t_r \sim \frac{\sigma^3 R^3}{G^2 m^2 N \log N} \sim \frac{N t_d}{\log N}, \quad (1)$$

where $t_d \sim R/\sigma$ is the dynamical time and the typical velocity $\sigma \sim (GmN/R)^{1/2}$ by the virial theorem. In plausible CDM models, the particle mass m is so small that the relaxation time is much larger than the age of the universe, so dark halos are collisionless. In FDM models, however, the effective mass m_{eff} of the quasiparticles is large enough that relaxation can be

* Hubble Fellow

important. Relaxation between the quasiparticles leads to the formation and growth of a central Bose–Einstein condensate or soliton, a process that we do not study here. Relaxation between the quasiparticles and macroscopic objects such as stars can heat, and therefore expand, the stellar system as it evolves toward equipartition with the quasiparticles. Relaxation between the quasiparticles and massive objects such as black holes or globular clusters can stall the inspiral of the massive object toward the center of the galaxy that is otherwise caused by dynamical friction from both baryonic and dark matter.

The goal of this paper is to place these physical arguments on a firm quantitative basis by analyzing the nature of the relaxation of classical particles, both test particles and massive objects, in an infinite FDM halo that is homogeneous in the mean. The paper is organized as follows. In Section 2, we derive the velocity diffusion coefficients for a zero-mass test particle traveling at constant velocity in a homogeneous halo with stochastic density fluctuations described by a correlation function. These results are used in Section 2.1 to re-derive the classical formulae for the diffusion coefficients in a gravitational N -body system and in Section 2.2 to derive the analogous formulae for an FDM halo. We find that there are remarkable parallels between the results of the two calculations. In Section 3, we consider the steady force acting on a massive object traveling through an FDM halo (dynamical friction), which completes the standard set of diffusion coefficients. We then turn in Section 4 to a brief discussion of two applications: the inspiral of a massive object into the galactic center by dynamical friction, which can be halted by relaxation at scales where the mass of the object becomes comparable to the mass of the FDM quasiparticles, and the expansion and heating of a stellar system such as a bulge embedded in an FDM halo. We summarize and conclude in Section 5.

1.1. The Coulomb logarithm

The factor $\log N$ in equation (1) is known as the Coulomb logarithm (Binney & Tremaine 2008). More generally, it is written as $\log \Lambda$, where $\Lambda \equiv b_{\max}/b_{\min}$ is the ratio between the maximum and minimum scales of the encounters that dominate the diffusion coefficients or relaxation time.

The calculations in this paper are for an infinite homogeneous system, for which we invoke the Jeans swindle, that is, we neglect any acceleration due to the homogeneous average density (Binney & Tremaine 2008). This assumption breaks down on scales larger than the Jeans length $(\sigma^2/G\rho)^{1/2}$, which for a finite system is comparable to the system’s radius R by the virial theorem. At scales much larger than R , the density is negligible so $b_{\max} \lesssim R$. In addition, if the system is centrally concentrated and the orbital size $r \ll R$, then the effects of encounters on a scale b with $r \ll b \ll R$ will average to zero.¹ Thus, we can set $b_{\max} \simeq \min(r, R)$.

In classical N -body systems composed of point particles of mass m_p , we set $b_{\min} \simeq b_{90} \equiv Gm_p/\sigma^2$; this is the impact parameter at which a typical particle is deflected by 90° . If the particles have a non-zero scale length ε , either because they represent star clusters or other sub-systems of non-zero size, or because they have been artificially “softened” to reduce integration errors, we set $b_{\min} \simeq \varepsilon$ (see Section 2 for more details). Finally, in modeling relaxation due to FDM quasiparticles we will show that it is appropriate to set the minimum scale to half of the typical de Broglie angular wavelength,² $b_{\min} \simeq \lambda_\sigma/2 \equiv \hbar/(2m_b\sigma)$.

These considerations lead us to define classical, softened, and FDM Coulomb factors:

$$\Lambda_{\text{cl}} \equiv \frac{b_{\max}}{b_{90}}, \quad \Lambda_{\text{soft}} \equiv \frac{b_{\max}}{\varepsilon}, \quad \Lambda_{\text{FDM}} \equiv \frac{2b_{\max}}{\lambda_\sigma}. \quad (2)$$

The precise value of Λ is uncertain by a factor of order unity because b_{\max} cannot be determined exactly from calculations in an infinite homogeneous medium.³ This ambiguity is only a minor concern in the common case where $\Lambda \gg 1$. Therefore, for clarity, we shall always express our formulae in terms of one of the three quantities in equation (2), even when the derivation yields a value for the argument of the log that differs from these by a factor of order unity.

2. DIFFUSION OF A TEST PARTICLE IN A FLUCTUATING DENSITY FIELD

In this section, we calculate the velocity diffusion coefficients for a zero-mass test particle embedded in a potential that exhibits stochastic fluctuations but is on average uniform in space and stationary in time. The stochastic fluctuations drive the evolution of the test particle’s velocity, and their spatial and temporal correlations determine the degree to which the test particle can respond to these fluctuations.⁴ Here we also restrict ourselves to the linear approximation, which for classical particles is equivalent to assuming that $\varepsilon \gg b_{90}$ in the notation of Section 1.1. This approximation is valid for most cases of interest involving FDM.

¹ This is not true for systems in which there is a global resonance, such as spherical or nearly Keplerian systems (e.g., Rauch & Tremaine 1996; Kocsis & Tremaine 2015). In such cases, “resonant relaxation” implies that the slow action associated with the global resonance relaxes much faster than the other actions.

² We distinguish between the typical de Broglie wavelength $\lambda_\sigma = \hbar/(m_b\sigma)$ and the typical de Broglie *angular* wavelength $\lambda_\sigma = \hbar/(m_b\sigma)$.

³ Accurate treatments of the diffusion coefficients in inhomogeneous equilibrium stellar systems require the analysis of orbital resonances (Tremaine & Weinberg 1984; Binney & Lacey 1988; Heyvaerts 2010; Chavanis 2012; Fouvy & Bar-Or 2018).

⁴ A similar approach was pioneered by Cohen (1975) who calculated the temporal and spatial correlations of the stochastic forces in a finite homogeneous stellar system.

Consider a time-dependent potential $\Phi(\mathbf{r}, t)$ with zero mean, $\langle \Phi(\mathbf{r}, t) \rangle = 0$, and stationary correlation function,

$$\langle \Phi(\mathbf{r}, t) \Phi(\mathbf{r}', t') \rangle = C_\Phi(\mathbf{r} - \mathbf{r}', t - t'); \quad (3)$$

here $\langle \cdot \rangle$ denotes an ensemble average, i.e., an average over all possible realizations of the potential. It is useful to write the potential in terms of its temporal and spatial Fourier transform, $\widehat{\Phi}(\mathbf{k}, \omega)$, defined by

$$\Phi(\mathbf{r}, t) = \iint \frac{d\mathbf{k}d\omega}{(2\pi)^4} \widehat{\Phi}(\mathbf{k}, \omega) e^{i\mathbf{k}\cdot\mathbf{r} - i\omega t}. \quad (4)$$

The correlation function of $\widehat{\Phi}(\mathbf{k}, \omega)$ is given by

$$\langle \widehat{\Phi}(\mathbf{k}, \omega) \widehat{\Phi}^*(\mathbf{k}', \omega') \rangle = (2\pi)^4 \widehat{C}_\Phi(\mathbf{k}, \omega) \delta(\omega - \omega') \delta(\mathbf{k} - \mathbf{k}'), \quad (5)$$

where $\widehat{C}_\Phi(\mathbf{k}, \omega)$ is the temporal and spatial Fourier transform of the potential correlation function $C_\Phi(\mathbf{r}, t)$.

Given the potential in equation (4), the acceleration of the test particle is

$$\dot{\mathbf{v}}(\mathbf{r}, t) = -\nabla\Phi(\mathbf{r}, t) = -i \iint \frac{\mathbf{k}d\mathbf{k}d\omega}{(2\pi)^4} \widehat{\Phi}(\mathbf{k}, \omega) e^{i\mathbf{k}\cdot\mathbf{r} - i\omega t}, \quad (6)$$

and its change in velocity over time t is given by

$$\Delta\mathbf{v}(t) = \int_0^t ds \dot{\mathbf{v}}[\mathbf{r}(s), s]. \quad (7)$$

As we assume that the mean force is zero, we can expand $\mathbf{r}(t)$ around the initial position and velocity,

$$\mathbf{r}(t) = \mathbf{r}_0 + \mathbf{v}_0 t + \int_0^t ds (t-s) \dot{\mathbf{v}}(\mathbf{r}_0 + \mathbf{v}_0 s, s) + \dots \quad (8)$$

Thus, the change in velocity is given by

$$\begin{aligned} \Delta\mathbf{v}(t) = & -i \iint \frac{\mathbf{k}d\mathbf{k}d\omega}{(2\pi)^4} \widehat{\Phi}(\mathbf{k}, \omega) e^{i\mathbf{k}\cdot\mathbf{r}_0} \int_0^t ds e^{i(\mathbf{k}\cdot\mathbf{v}_0 - \omega)s} \\ & + i \iint \frac{\mathbf{k}d\mathbf{k}d\omega}{(2\pi)^4} \iint \frac{\mathbf{k}\cdot\mathbf{k}'d\mathbf{k}'d\omega'}{(2\pi)^4} \widehat{\Phi}(\mathbf{k}, \omega) \widehat{\Phi}^*(\mathbf{k}', \omega') e^{i(\mathbf{k}-\mathbf{k}')\cdot\mathbf{r}_0} \int_0^t ds e^{i(\mathbf{k}\cdot\mathbf{v}_0 - \omega)s} \int_0^s ds' (s-s') e^{-i(\mathbf{k}'\cdot\mathbf{v}_0 - \omega')s'}, \end{aligned} \quad (9)$$

in which we have kept only terms up to second order in $\widehat{\Phi}(\mathbf{k}, \omega)$.

To proceed forward, we assume that changes in velocity result from the accumulation of many small increments. As a result, the velocity evolution can be described by a Fokker–Planck equation in which the first and second diffusion coefficients are the first and second moments of the transition probability, namely $D[\Delta v_i] = \langle \Delta v_i(T) \rangle / T$ and $D[\Delta v_i \Delta v_j] = \langle \Delta v_i(T) \Delta v_j(T) \rangle / T$, where $\Delta v_i(T)$ is the change in velocity component i over a time T . This is equivalent to ignoring higher moments of the transition probability (e.g., Hénon 1960; Risken 1989) and is usually a good assumption if the first and second moments of the transition probability are finite.

Therefore, the diffusion coefficients are given by⁵

$$D[\Delta v_i] = \frac{1}{2} \sum_j \frac{\partial}{\partial v_j} \iint \frac{d\mathbf{k}d\omega}{(2\pi)^3} k_i k_j \widehat{C}_\Phi(\mathbf{k}, \omega) K_T(\omega - \mathbf{k} \cdot \mathbf{v}), \quad (10)$$

and

$$D[\Delta v_i \Delta v_j] = \iint \frac{d\mathbf{k}d\omega}{(2\pi)^3} k_i k_j \widehat{C}_\Phi(\mathbf{k}, \omega) K_T(\omega - \mathbf{k} \cdot \mathbf{v}), \quad (11)$$

where

$$K_T(\omega) \equiv \frac{1}{2\pi T} \int_0^T \int_0^T ds ds' e^{i\omega(s-s')} = \frac{1 - \cos(\omega T)}{\pi \omega^2 T}, \quad (12)$$

⁵ In deriving the first of these equations, we have made use of the fact that $\Phi(\mathbf{r}, t)$ is real, so $\widehat{C}_\Phi(-\mathbf{k}, -\omega) = \widehat{C}_\Phi(\mathbf{k}, \omega)$ for real ω and \mathbf{k} .

is the finite-time kernel, which is normalized such that $\int d\omega K_T(\omega) = 1$. In the limit $T \rightarrow \infty$, $K_T(\omega) \rightarrow \delta(\omega)$ and $D[\Delta v_i \Delta v_j]$ becomes time-independent, and the process is diffusive. On short timescales, $K_T \rightarrow T/(2\pi)$, the process is ballistic, and $D[\Delta v_i \Delta v_j] \simeq \langle \dot{v}_i \dot{v}_j \rangle T$ describes the instantaneous coherent (in time) force acting on the test particle.

Equations (10) and (11) satisfy the relation

$$D[\Delta v_i] = \frac{1}{2} \sum_j \frac{\partial}{\partial v_j} D[\Delta v_i \Delta v_j], \quad (13)$$

which is the fluctuation-dissipation relation for a zero-mass test particle (e.g., Binney & Lacey 1988; Binney & Tremaine 2008).⁶

We now assume that there is a finite correlation time T_c such that $C_\Phi(\mathbf{r}, t) \rightarrow 0$ for $|t| \gg T_c$, and that this correlation time is much shorter than any other time of interest. This assumption allows us to take the limit $T \rightarrow \infty$, in which the kernel $K_T(\omega)$ can be approximated as a delta function. Equations (10) and (11) then read

$$D_i = D[\Delta v_i] = \frac{1}{2} \sum_j \frac{\partial}{\partial v_j} \int \frac{d\mathbf{k}}{(2\pi)^3} k_i k_j \hat{C}_\Phi(\mathbf{k}, \mathbf{k} \cdot \mathbf{v}), \quad (14)$$

$$D_{ij} = D[\Delta v_i \Delta v_j] = \int \frac{d\mathbf{k}}{(2\pi)^3} k_i k_j \hat{C}_\Phi(\mathbf{k}, \mathbf{k} \cdot \mathbf{v}). \quad (15)$$

Under these approximations, the probability distribution of the velocity of a test particle, $P(\mathbf{v}, t)$, is governed by the Fokker-Planck equation

$$\frac{\partial P(\mathbf{v}, t)}{\partial t} = - \sum_i \frac{\partial}{\partial v_i} [D_i P(\mathbf{v}, t)] + \frac{1}{2} \sum_{ij} \frac{\partial^2}{\partial v_i \partial v_j} [D_{ij} P(\mathbf{v}, t)] = \frac{1}{2} \sum_{ij} \frac{\partial}{\partial v_i} \left[D_{ij} \frac{\partial P(\mathbf{v}, t)}{\partial v_j} \right], \quad (16)$$

where the last equality is derived using equation (13).

We now specialize to the case in which the potential fluctuations arise from density fluctuations $\rho(\mathbf{r}, t)$ around a mean field density ρ_p , so $\langle \rho(\mathbf{r}, t) \rangle = 0$. Assuming that these fluctuations are a stationary homogeneous random field, the correlation function of the density fluctuations can be written as

$$\langle \rho(\mathbf{r}, t) \rho(\mathbf{r}', t') \rangle = C_\rho(\mathbf{r} - \mathbf{r}', t - t'). \quad (17)$$

The potential fluctuations associated with the density fluctuations $\rho(\mathbf{r}, t)$ are given by the Fourier transform of Poisson's equation, $\hat{\Phi}(\mathbf{k}, \omega) = -4\pi G \hat{\rho}(\mathbf{k}, \omega)/k^2$, $k = |\mathbf{k}|$, and the Fourier transforms of the correlation functions are related by

$$\hat{C}_\Phi(\mathbf{k}, \omega) = \frac{16\pi^2 G^2}{k^4} \hat{C}_\rho(\mathbf{k}, \omega). \quad (18)$$

The diffusion coefficients, equations (14) and (15), become

$$D_i = \frac{G^2}{\pi} \sum_j \frac{\partial}{\partial v_j} \int d\mathbf{k} \frac{k_i k_j}{k^4} \hat{C}_\rho(\mathbf{k}, \mathbf{k} \cdot \mathbf{v}), \quad (19)$$

$$D_{ij} = \frac{2G^2}{\pi} \int d\mathbf{k} \frac{k_i k_j}{k^4} \hat{C}_\rho(\mathbf{k}, \mathbf{k} \cdot \mathbf{v}). \quad (20)$$

2.1. Classical two-body relaxation

We now use the results from the preceding discussion to obtain the diffusion coefficients for a zero-mass test particle interacting with an infinite, homogeneous system of classical ‘‘field’’ particles of individual mass m_p , characterized by a distribution function (DF) $F_p(\mathbf{v})$. Here, the DF is normalized such that $\int d\mathbf{v} F_p(\mathbf{v})$ is the mass density ρ_p , and we ignore the self-gravity of the particles, considering only the gravitational forces that they exert on the test particle. This is the system examined in the classic work of Chandrasekhar (1942, 1943).

Given our assumptions, each field particle travels on a straight line at constant velocity. Then, the density fluctuations around the mean density ρ_p are given by

$$\rho(\mathbf{r}, t) = m_p \sum_n \delta(\mathbf{r} - \mathbf{r}_n - \mathbf{v}_n t) - \rho_p, \quad (21)$$

⁶ This derivation is more general than the one in Binney & Tremaine (2008), which requires that the distribution function of the particles that cause the potential fluctuations is isotropic in velocity space.

where $(\mathbf{r}_n, \mathbf{v}_n)$ stands for the position and velocity of the field particle n at time $t = 0$. The associated density correlation function is

$$C_\rho(\mathbf{r} - \mathbf{r}', t - t') = \langle \rho(\mathbf{r}, t) \rho(\mathbf{r}', t') \rangle = m_p \int d\mathbf{v} \delta[\mathbf{r} - \mathbf{r}' - \mathbf{v}(t - t')] F_p(\mathbf{v}), \quad (22)$$

and its temporal and spatial Fourier transform is

$$\widehat{C}_\rho(\mathbf{k}, \omega) = 2\pi m_p \int d\mathbf{v}' \delta(\mathbf{k} \cdot \mathbf{v}' - \omega) F_p(\mathbf{v}'). \quad (23)$$

From equations (19) and (20), we obtain the first and second-order diffusion coefficients,

$$\begin{aligned} D_i &= 2G^2 m_p \log \Lambda \int d\widehat{\mathbf{k}} \widehat{k}_i \int d\mathbf{v}' \widehat{\mathbf{k}} \cdot \frac{\partial}{\partial \mathbf{v}} \delta[\widehat{\mathbf{k}} \cdot (\mathbf{v}' - \mathbf{v})] F_p(\mathbf{v}') \\ &= 2G^2 m_p \log \Lambda \frac{\partial}{\partial v_i} \int d\widehat{\mathbf{k}} \int d\mathbf{v}' \delta[\widehat{\mathbf{k}} \cdot (\mathbf{v}' - \mathbf{v})] F_p(\mathbf{v}') \\ &= 4\pi G^2 m_p \log \Lambda \frac{\partial}{\partial v_i} \int d\mathbf{v}' \frac{F_p(\mathbf{v}')}{|\mathbf{v} - \mathbf{v}'|}, \end{aligned} \quad (24)$$

and

$$\begin{aligned} D_{ij} &= 4G^2 m_p \log \Lambda \int d\widehat{\mathbf{k}} \widehat{k}_i \widehat{k}_j \int d\mathbf{v}' \delta[\widehat{\mathbf{k}} \cdot (\mathbf{v}' - \mathbf{v})] F_p(\mathbf{v}') \\ &= 2G^2 m_p \log \Lambda \frac{\partial^2}{\partial v_i \partial v_j} \int d\widehat{\mathbf{k}} \int d\mathbf{v}' |\widehat{\mathbf{k}} \cdot (\mathbf{v}' - \mathbf{v})| F_p(\mathbf{v}') \\ &= 4\pi G^2 m_p \log \Lambda \frac{\partial^2}{\partial v_i \partial v_j} \int d\mathbf{v}' |\mathbf{v} - \mathbf{v}'| F_p(\mathbf{v}'), \end{aligned} \quad (25)$$

where $\widehat{\mathbf{k}} \equiv \mathbf{k}/|\mathbf{k}|$. Here, $\log \Lambda = \int dk/k = \log k_{\max}/k_{\min}$ is the Coulomb logarithm (Section 1.1), because we can identify $1/k_{\min}$ and $1/k_{\max}$ as the maximum and minimum scales b_{\max} and b_{\min} to within factors of order unity. To obtain equations (24) and (25), we used the relation

$$\frac{\partial}{\partial x_{j_1}} \dots \frac{\partial}{\partial x_{j_\ell}} \int d\widehat{\mathbf{k}} \widehat{k}_{i_1} \dots \widehat{k}_{i_n} \delta(\widehat{\mathbf{k}} \cdot \mathbf{x}) = \frac{\partial}{\partial x_{i_1}} \dots \frac{\partial}{\partial x_{i_n}} \int d\widehat{\mathbf{k}} \widehat{k}_{j_1} \dots \widehat{k}_{j_\ell} \Delta_{n-\ell}(\widehat{\mathbf{k}} \cdot \mathbf{x}), \quad (26)$$

where

$$\Delta_n(x) = \begin{cases} \frac{1}{2(n-1)!} \frac{x^n}{|x|}, & n > 0, \\ \delta^{(n)}(x), & n \leq 0, \end{cases} \quad (27)$$

is the n th integral (derivative) of the Dirac delta function $\delta(x)$.

The diffusion coefficients in equations (24) and (25) are identical to the standard diffusion coefficients (Rosenbluth et al. 1957; see also Chavanis 2013) for a zero-mass test particle in an infinite homogeneous medium, up to the usual ambiguity in the precise definition of the Coulomb logarithm.

Plugging the diffusion coefficients into the Fokker-Planck equation (16), we obtain the (homogeneous) Landau equation (Landau 1936) for a zero-mass test particle,

$$\frac{\partial P(\mathbf{v}, t)}{\partial t} = 2G^2 m_p \sum_{ij} \frac{\partial}{\partial v_i} \int d\mathbf{k} \int d\mathbf{v}' \frac{k_i k_j}{k^4} \delta[\mathbf{k} \cdot (\mathbf{v} - \mathbf{v}')] F_p(\mathbf{v}') \frac{\partial}{\partial v_j} P(\mathbf{v}, t). \quad (28)$$

See Chavanis (2013) for the historical connection between this equation and the later treatments of Chandrasekhar (1942, 1943) and Rosenbluth et al. (1957).

For a Maxwellian velocity distribution,

$$F_p(\mathbf{v}) = \frac{\rho_p}{(2\pi\sigma^2)^{3/2}} e^{-v^2/(2\sigma^2)}, \quad (29)$$

with $v = |\mathbf{v}|$; the integral expressions for the diffusion coefficients, equations (24) and (25), can be evaluated explicitly. The diffusion coefficients in the directions parallel and perpendicular to the test-particle velocity are (Binney & Tremaine 2008)

$$D[\Delta v_{\parallel}] = -\frac{4\pi G^2 \rho_p m_p \log \Lambda}{\sigma^2} \mathbb{G}(X) \quad (30)$$

$$D[(\Delta v_{\parallel}^2)] = \frac{4\sqrt{2}\pi G^2 \rho_p m_p \log \Lambda}{\sigma} \frac{\mathbb{G}(X)}{X}, \quad (31)$$

$$D[(\Delta \mathbf{v}_{\perp})^2] = \frac{4\sqrt{2}\pi G^2 \rho_p m_p \log \Lambda}{\sigma} \left[\frac{\text{erf}(X) - \mathbb{G}(X)}{X} \right], \quad (32)$$

where $X \equiv v/\sqrt{2}\sigma$ and

$$\mathbb{G}(X) \equiv \frac{1}{2X^2} \left[\text{erf}(X) - \frac{2X}{\sqrt{\pi}} e^{-X^2} \right]. \quad (33)$$

The Cartesian diffusion coefficients are then

$$D_i = \frac{v_i}{v} D[\Delta v_{\parallel}], \quad (34)$$

$$D_{ij} = \frac{v_i v_j}{v^2} \left\{ D[(\Delta v_{\parallel})^2] - \frac{1}{2} D[(\Delta \mathbf{v}_{\perp})^2] \right\} + \frac{1}{2} \delta_{ij} D[(\Delta \mathbf{v}_{\perp})^2]. \quad (35)$$

Until now, we have considered a classical system composed of point-like particles. We now generalize this to a system of extended field particles, where each particle has a density profile $\rho_n(r) = m_p W_{\varepsilon}(r)$ with a scale length ε and $\int d\mathbf{r} W_{\varepsilon}(|\mathbf{r}|) = 1$. The density fluctuations are now given by $\rho(\mathbf{r}, t) = m_p \sum_n W_{\varepsilon}(|\mathbf{r} - \mathbf{r}_n - \mathbf{v}_n t|) - \rho_p$, and their correlation function is

$$C_{\rho}(\mathbf{r}, t) = m_p \int d\mathbf{v} \int d\mathbf{r}' W_{\varepsilon}(\mathbf{r} - \mathbf{r}' - \mathbf{v}t) W_{\varepsilon}(\mathbf{r}') F_p(\mathbf{v}). \quad (36)$$

This approach is equivalent to using a softened version of Poisson's equation,

$$\Phi_{\varepsilon}(\mathbf{r}, t) = -G \int d\mathbf{r}' \int d\mathbf{r}'' \frac{\rho(\mathbf{r}'', t)}{|\mathbf{r} - \mathbf{r}'|} W_{\varepsilon}(|\mathbf{r}' - \mathbf{r}''|), \quad (37)$$

where $W_{\varepsilon}(r)$ is the softening kernel. As discussed in Section 1.1, this softening cures the divergence in the Coulomb logarithm at small scales (large wavenumbers). The Fourier transform of the softened potential is $\widehat{\Phi}_{\varepsilon}(\mathbf{k}, \omega) = -4\pi G \widehat{\rho}(\mathbf{k}, \omega) \widehat{W}_{\varepsilon}(k)/k^2$. The diffusion coefficient is the same as in equation (25), but now the Coulomb logarithm is

$$\log \Lambda_{\text{soft}} = \int_{k_{\min}}^{k_{\max}} \frac{dk}{k} |\widehat{W}_{\varepsilon}(k)|^2. \quad (38)$$

If we take the density kernel to be Gaussian,

$$W_{\varepsilon}(r) = \frac{1}{(2\pi\varepsilon^2)^{3/2}} e^{-\frac{1}{2}r^2/\varepsilon^2}, \quad \widehat{W}_{\varepsilon}(\mathbf{k}) = e^{-\frac{1}{2}k^2\varepsilon^2}, \quad (39)$$

then we can let $k_{\max} \rightarrow \infty$ and obtain

$$\log \Lambda_{\text{soft}} = \frac{1}{2} \Gamma(0, k_{\min}^2 \varepsilon^2), \quad (40)$$

where $\Gamma(n, x) = \int_x^{\infty} t^{n-1} e^{-t} dt$ is the ‘‘upper’’ incomplete Gamma function. In the limit $k_{\min} \varepsilon \rightarrow 0$, this expression is equivalent to $\log \Lambda_{\text{soft}} = -\log(k_{\min} \varepsilon) - \frac{1}{2} \gamma_E + \mathcal{O}(k_{\min} \varepsilon)^2 = \log(b_{\max}/\varepsilon) + \mathcal{O}(1)$ with γ_E the Euler constant. This result is consistent with the second of equations (2).

For a Gaussian density kernel and a Maxwellian DF, the density correlation function (eq. 36) is

$$C_{\rho}(\mathbf{r}, t) = \frac{m_p \rho_b}{8\pi^{3/2} \varepsilon^3 \left[1 + (\sigma t / \sqrt{2}\varepsilon)^2 \right]^{3/2}} \exp \left[-\frac{(r/2\varepsilon)^2}{1 + (\sigma t / \sqrt{2}\varepsilon)^2} \right]. \quad (41)$$

The force correlation function $\langle \mathbf{F}(\mathbf{r}, t) \cdot \mathbf{F}(\mathbf{r}', t') \rangle = C_F(\mathbf{r} - \mathbf{r}', t - t')$ is given by

$$C_F(\mathbf{r}, t) = 4\pi G^2 \int d\mathbf{r}' \frac{C_{\rho}(\mathbf{r}', t)}{|\mathbf{r} - \mathbf{r}'|} = \frac{4\pi G^2 m_p \rho_b}{r} \text{erf} \left[\frac{r/2\varepsilon}{\sqrt{1 + (\sigma t / \sqrt{2}\varepsilon)^2}} \right], \quad (42)$$

which in the limit $\varepsilon \rightarrow 0$ asymptotes to $4\pi G^2 m_p \rho_b r^{-1} \text{erf}[r/(\sqrt{2}\sigma t)]$ (Cohen 1975, eq. 15).

2.2. Relaxation by fuzzy dark matter

In this section, we describe how the stochastic density fluctuations that arise inevitably in an FDM halo lead to the diffusion of the velocity of a zero-mass test particle.

The wavefunction $\psi(\mathbf{r}, t)$ of the FDM is governed by the Schrödinger–Poisson system (Ruffini & Bonazzola 1969)

$$i\hbar \frac{\partial}{\partial t} \psi(\mathbf{r}, t) = -\frac{\hbar^2}{2m_b} \nabla^2 \psi(\mathbf{r}, t) + m_b \Phi(\mathbf{r}, t) \psi(\mathbf{r}, t), \quad (43)$$

$$\nabla^2 \Phi(\mathbf{r}, t) = 4\pi G |\psi(\mathbf{r}, t)|^2. \quad (44)$$

Here, m_b is the mass of the FDM particle, $\Phi(\mathbf{r}, t)$ is the gravitational potential, and we have assumed that the wavefunction is normalized such that $|\psi(\mathbf{r}, t)|^2$ is the mass density.

To parallel our discussion of relaxation in a system of classical particles in the preceding subsection, we assume that the self-gravity of the FDM can be ignored when considering the interaction of FDM with a classical test particle. This assumption is similar to the Jeans swindle and is valid when the typical de Broglie wavelength is much smaller than the scale of the system. In this case, the FDM wavefunction can be expanded as a collection of plane waves,

$$\psi(\mathbf{r}, t) = \int d\mathbf{k} \varphi(\mathbf{k}) e^{i\mathbf{k}\cdot\mathbf{r} - i\omega(k)t}, \quad (45)$$

where

$$\omega(k) = \frac{\hbar k^2}{2m_b}. \quad (46)$$

We assume that the ensemble averages of $\varphi(\mathbf{k})$ satisfy

$$\langle \varphi(\mathbf{k}) \rangle = 0, \quad \langle \varphi(\mathbf{k}) \varphi(\mathbf{k}') \rangle = 0 \quad \text{for } \mathbf{k} \neq \mathbf{k}'. \quad (47)$$

These equations are satisfied if each plane wave has a random phase, as is expected if they arrive in the vicinity of the test particle from large distances and different directions. We also assume that

$$\langle \varphi(\mathbf{k}) \varphi^*(\mathbf{k}') \rangle = f_k(\mathbf{k}) \delta(\mathbf{k} - \mathbf{k}'). \quad (48)$$

where $f_k(\mathbf{k})$ is a DF defined such that the mean or ensemble-average mass density in the volume $d\mathbf{k}$ around \mathbf{k} is $f_k(\mathbf{k})d\mathbf{k}$.

These assumptions are only valid when the typical de Broglie angular wavelength λ_σ is much larger than the typical distance between FDM particles, $d = (m_b/\rho_b)^{1/3}$. Therefore, the results in the remainder of this section do not reduce to the classical diffusion coefficients in the classical limit where $\hbar \rightarrow 0$. In the Appendix A, we generalize our derivation to include the classical limit. There, we show that $\lambda_\sigma > d$ when the FDM particle mass exceeds $m_s \approx (\rho_b \hbar^3 / \sigma^3)^{1/4}$, a few tens of eV in a typical galaxy. For $m_b \gg m_s$ the diffusion coefficients become the classical ones, although the system itself is not yet in the classical limit. Classical behavior requires that the position uncertainty after a dynamical time T_d be small compared to the distance between particles or $m_b \gg m_c$, where $m_c \approx (\hbar T_d / 2)^{3/5} \rho_b^{2/5}$, about 10^{16} eV in a typical galaxy. For any reasonable dark-matter particle mass, the “classical” contribution to the relaxation is of no importance.

Note that although \hbar is present in the wave function and the dispersion relation (eqs. 45 and 46) and thus will appear in many of the following formulas, the following derivations can be understood entirely as a classical field theory: the only trace of the quantum nature of the waves is in the quadratic dispersion relation (see eq. 46), which is rare in classical systems.

The density fluctuations of the FDM field are given by $\rho(\mathbf{r}, t) = |\psi(\mathbf{r}, t)|^2 - \rho_b$, where the mean FDM density is $\rho_b = \langle |\psi(\mathbf{r}, t)|^2 \rangle = \int d\mathbf{k} f_k(\mathbf{k})$. From equation (45), we obtain

$$\rho(\mathbf{r}, t) = \int d\mathbf{k} \int d\mathbf{k}' \varphi(\mathbf{k}) \varphi^*(\mathbf{k}') e^{i(\mathbf{k}-\mathbf{k}')\cdot\mathbf{r} - i[\omega(k) - \omega(k')]t} - \rho_b. \quad (49)$$

The density correlation function and its Fourier transform are

$$C_\rho(\mathbf{r}, t) = \int d\mathbf{k} \int d\mathbf{k}' f_k(\mathbf{k}) f_k(\mathbf{k}') e^{i(\mathbf{k}-\mathbf{k}')\cdot\mathbf{r} - i[\omega(k) - \omega(k')]t}, \quad (50)$$

$$\hat{C}_\rho(\mathbf{k}, \omega) = (2\pi)^4 \int d\mathbf{k}' \int d\mathbf{k}'' f_k(\mathbf{k}) f_k(\mathbf{k}'') \delta(\mathbf{k} - \mathbf{k}' + \mathbf{k}'') \delta[\omega - \omega(k') + \omega(k'')]. \quad (51)$$

Here, we used equations (47) and (48) to obtain

$$\begin{aligned} \langle \varphi(\mathbf{k}_1) \varphi^*(\mathbf{k}_2) \varphi^*(\mathbf{k}_3) \varphi(\mathbf{k}_4) \rangle &= f_k(\mathbf{k}_1) f_k(\mathbf{k}_3) \delta(\mathbf{k}_1 - \mathbf{k}_2) \delta(\mathbf{k}_3 - \mathbf{k}_4) \\ &\quad + f_k(\mathbf{k}_1) f_k(\mathbf{k}_2) \delta(\mathbf{k}_1 - \mathbf{k}_3) \delta(\mathbf{k}_2 - \mathbf{k}_4). \end{aligned} \quad (52)$$

Each plane wave travels with velocity $\mathbf{v} = \hbar \mathbf{k} / m_b$, and its velocity DF is given by $F_b(\mathbf{v}) d\mathbf{v} = f_k(\mathbf{k}) d\mathbf{k}$. As a result, equation (51) can be written as

$$\widehat{C}_\rho(\mathbf{k}, \omega) = (2\pi)^4 \int d\mathbf{v}_1 \int d\mathbf{v}_2 F_b(\mathbf{v}_1) F_b(\mathbf{v}_2) \delta\left(\mathbf{k} - \frac{2m_b}{\hbar} \mathbf{v}_d\right) \delta\left(\omega - \frac{2m_b}{\hbar} \mathbf{v}_c \cdot \mathbf{v}_d\right), \quad (53)$$

in which we have introduced the velocities $\mathbf{v}_c = (\mathbf{v}_1 + \mathbf{v}_2)/2$ and $\mathbf{v}_d = (\mathbf{v}_1 - \mathbf{v}_2)/2$. Note that in this case the spatial correlation is associated with the velocity difference, while in the classical case it is associated with the distance that a field particle travels over time t (eq. 23). Therefore, truncating the integrals at large and small scales is equivalent to truncating the velocity difference.

Using equations (20) and (53), we obtain the diffusion coefficient for the test particle

$$\begin{aligned} D_{ij} &= \frac{32\pi^3 G^2 \hbar^3}{m_b^3} \int d\mathbf{v}_d \int d\mathbf{v}_c \frac{v_d^i v_d^j}{v_d^5} F_b(\mathbf{v}_c + \mathbf{v}_d) F_b(\mathbf{v}_c - \mathbf{v}_d) \delta(\widehat{\mathbf{v}}_d \cdot \mathbf{v} - \widehat{\mathbf{v}}_d \cdot \mathbf{v}_c) \\ &= \frac{16\pi^3 G^2 \hbar^3}{m_b^3} \frac{\partial^2}{\partial v_i \partial v_j} \int d\mathbf{v}_d \int d\mathbf{v}_c F_b(\mathbf{v}_c + \mathbf{v}_d) F_b(\mathbf{v}_c - \mathbf{v}_d) \frac{|\widehat{\mathbf{v}}_d \cdot \mathbf{v} - \widehat{\mathbf{v}}_d \cdot \mathbf{v}_c|}{v_d^3}, \end{aligned} \quad (54)$$

where $\widehat{\mathbf{v}}_d$ is the unit vector in the direction of \mathbf{v}_d . The diffusion coefficient D_i can be obtained from D_{ij} using the fluctuation-dissipation relation (eq. 13).

The integrals over \mathbf{v}_d diverge logarithmically as $|\mathbf{v}_d| \rightarrow 0$. Therefore, we cut off the integration when $|\mathbf{v}_d| < v_{d,\min}$. This cut-off arises naturally from the wave nature of FDM: because $v = \hbar k / m_b$ and we ignore wavenumbers smaller than $k_{\min} = 1/b_{\max}$, we should also ignore velocities $v \lesssim \hbar / (m_b b_{\max})$. More precisely, we set $v_{d,\min} = \hbar / (2m_b b_{\max}) = \sigma \lambda_\sigma / (2b_{\max})$, where $\lambda_\sigma = \hbar / (m_b \sigma)$ is the typical de Broglie angular wavelength. Furthermore, the integral is dominated by the region $|\mathbf{v}_d| \ll |\mathbf{v}_c|$, so we may also cut off the integration when $|\mathbf{v}_d| > v_{d,\max}$, where $v_{d,\max} \lesssim \sigma$, and approximate $F_b(\mathbf{v}_c \pm \mathbf{v}_d)$ by $F_b(\mathbf{v}_c)$.

If we write $\mathbf{v}_d \equiv v_d \widehat{\mathbf{k}}$, the first of equations (54) simplifies to

$$\begin{aligned} D_{ij} &= \frac{32\pi^3 G^2 \hbar^3}{m_b^3} \log \Lambda_{\text{FDM}} \int d\widehat{\mathbf{k}} \widehat{k}_i \widehat{k}_j \int d\mathbf{v}' F_b^2(\mathbf{v}') \delta[\widehat{\mathbf{k}} \cdot (\mathbf{v} - \mathbf{v}')] \\ &= 4G^2 m_{\text{eff}} \log \Lambda_{\text{FDM}} \int d\widehat{\mathbf{k}} \widehat{k}_i \widehat{k}_j \int d\mathbf{v}' \delta[\widehat{\mathbf{k}} \cdot (\mathbf{v} - \mathbf{v}')] F_{\text{eff}}(\mathbf{v}'), \end{aligned} \quad (55)$$

and

$$D_i = 4\pi G^2 m_{\text{eff}} \log \Lambda_{\text{FDM}} \frac{\partial}{\partial v_i} \int d\mathbf{v}' \frac{F_{\text{eff}}(\mathbf{v}')}{|\mathbf{v} - \mathbf{v}'|}. \quad (56)$$

Here, $\log \Lambda_{\text{FDM}} = \log(v_{d,\max}/v_{d,\min}) = \log(2b_{\max}/\lambda_\sigma) + \mathcal{O}(1)$, consistent with the third of equations (2). We have also defined a new, effective DF,

$$F_{\text{eff}}(\mathbf{v}) = \frac{\int d\mathbf{v} F_b(\mathbf{v})}{\int d\mathbf{v} F_b^2(\mathbf{v})} F_b^2(\mathbf{v}), \quad (57)$$

normalized such that $\int d\mathbf{v} F_{\text{eff}}(\mathbf{v}) = \rho_b$, and an effective mass,

$$m_{\text{eff}} = \frac{(2\pi\hbar)^3 \int d\mathbf{v} F_b^2(\mathbf{v})}{m_b^3 \int d\mathbf{v} F_b(\mathbf{v})}. \quad (58)$$

The diffusion coefficients in equations (56) and (55) are identical to the diffusion coefficients in equations (24) and (25) for classical particles, except that the particle mass m_p is replaced by the effective mass m_{eff} , the velocity DF $F_b(\mathbf{v})$ is replaced by the effective DF $F_{\text{eff}}(\mathbf{v})$, and the Coulomb logarithm $\log \Lambda$ is modified to $\log \Lambda_{\text{FDM}}$. In effect, the halo acts as if it were composed of quasiparticles with a mass m_{eff} that depends on the local halo density and velocity distribution. These results provide a simple recipe for computing the diffusion coefficients for a zero-mass test particle in an FDM halo.

For the Maxwellian velocity distribution (eq. 29), the integrations in equations (54)–(58) can be carried out explicitly. The effective DF is a Maxwellian with the same density and a velocity dispersion $\sigma_{\text{eff}} = \sigma/\sqrt{2}$. The effective mass is

$$m_{\text{eff}} = \frac{\pi^{3/2} \hbar^3 \rho_{\text{b}}}{m_{\text{b}}^3 \sigma^3} = \rho_{\text{b}} (f \lambda_{\sigma})^3, \quad (59)$$

where $\lambda_{\sigma} = h/(m_{\text{b}}\sigma)$ is the typical de Broglie wavelength and $f = 1/(2\sqrt{\pi}) = 0.282$. Moreover, by evaluating the integral in equation (54) for a Maxwellian, we can sharpen our estimate of the Coulomb logarithm. We find (cf. eq. 40)

$$\begin{aligned} \log \Lambda_{\text{FDM}} &= \int_{v_{d,\min}}^{\infty} \frac{dv}{v} e^{-v^2/\sigma^2} = \frac{1}{2} \Gamma(0, v_{d,\min}^2/\sigma^2) \\ &= \log(\sigma/v_{d,\min}) - \frac{1}{2} \gamma_E + \text{O}(v_{d,\min}/\sigma)^2. \end{aligned} \quad (60)$$

Substituting $v_{d,\min} \simeq \sigma \lambda_{\sigma}/(2b_{\text{max}})$ (see the paragraph preceding eq. 55),

$$\log \Lambda_{\text{FDM}} = \frac{1}{2} \Gamma(0, \frac{1}{4} \lambda_{\sigma}^2/b_{\text{max}}^2) = \log(2b_{\text{max}}/\lambda_{\sigma}) - \frac{1}{2} \gamma_E + \text{O}(\lambda_{\sigma}/b_{\text{max}})^2, \quad (61)$$

which is equivalent to the classical case with a softening scale $\varepsilon = \lambda_{\sigma}/2$ (cf. eq. 40).

As the density correlation function determines the diffusion coefficients (cf. eqs. 19 and 20), it is instructive to compare the FDM correlation function to a classical one. For a Maxwellian velocity distribution, the density correlation function (eq. 50) is given by

$$C_{\rho}(\mathbf{r}, t) = \frac{\rho_{\text{b}}^2}{[1 + (\sigma t/\lambda_{\sigma})^2]^{3/2}} \exp\left[-\frac{(r/\lambda_{\sigma})^2}{1 + (\sigma t/\lambda_{\sigma})^2}\right]. \quad (62)$$

This result can be compared with numerical simulations of FDM halos (e.g., Lin et al. 2018). Comparing this result with equation (41), we see that the density correlation function is the same as that of a classical system having a Maxwellian DF with velocity dispersion $\sigma_{\text{p}} = \sigma_{\text{eff}}$, a Gaussian density kernel with a softening $\varepsilon = \lambda_{\sigma}/2$, and individual particle mass $m_{\text{p}} = m_{\text{eff}}$. Note that uncertainties about the Coulomb logarithm are absent from equation (62).

These results verify the qualitative picture of relaxation in FDM halos presented by Hui et al. (2017), who assumed that the diffusion coefficients were the same as those of a halo of classical particles with the same velocity dispersion and effective mass $\rho_{\text{b}}(f_{\text{H}}\lambda_{\sigma})^3$, with $f_{\text{H}} \simeq 0.5$. The calculations in this section show that the actual value of f_{H} is between 0.224 and 0.399 depending on the velocity of the test particle and on which of the diffusion coefficient is being evaluated; thus, the diffusion coefficients and relaxation rates are between 2 and 11 times smaller than those assumed by Hui et al. (2017). The formulation here, which defines the effective mass for a distribution with dispersion $\sigma_{\text{eff}} = \sigma/\sqrt{2}$, is both simpler and more accurate.

To estimate m_{eff} , one can assume that the density is related to the radius r and the one-dimensional velocity dispersion σ or the circular speed v_{c} as in a singular isothermal sphere,

$$\rho_{\text{b}}(r) = \frac{\sigma^2}{2\pi G r^2} = \frac{v_{\text{c}}^2}{4\pi G r^2}, \quad (63)$$

which leads to

$$m_{\text{eff}} = \frac{\pi^{1/2} \hbar^3}{2^{1/2} G m_{\text{b}}^3 v_{\text{c}} r^2} = 1.03 \times 10^7 M_{\odot} \left(\frac{r}{1 \text{ kpc}}\right)^{-2} \left(\frac{m_{\text{b}}}{10^{-22} \text{ eV}}\right)^{-3} \left(\frac{v_{\text{c}}}{200 \text{ km s}^{-1}}\right)^{-1}, \quad (64)$$

and the typical de Broglie wavelength is

$$\lambda_{\sigma} = \frac{h}{m_{\text{b}}\sigma} = 0.85 \text{ kpc} \left(\frac{m_{\text{b}}}{10^{-22} \text{ eV}}\right)^{-1} \left(\frac{v_{\text{c}}}{200 \text{ km s}^{-1}}\right)^{-1}. \quad (65)$$

3. DYNAMICAL FRICTION

In the previous section, we calculated the stochastic velocity changes of a massless particle moving through a homogeneous FDM background. In this section, we consider the additional contribution to the velocity change for a particle of non-zero mass.

A massive particle moving through the FDM field creates a gravitational wake behind it that induces a frictional force proportional to the mass of the particle. We will call this force dynamical friction; it is distinct from the velocity drift described by the diffusion coefficient D_i or $D[\Delta v_{\parallel}]$ (eq. 56), which is independent of the test star's mass.⁷

⁷ In the literature, it is common to define dynamical friction as the sum of both drift terms.

The frictional force on a point object of mass m_t traveling at velocity \mathbf{v}_t through a plane wave with velocity $\mathbf{v} = \hbar\mathbf{k}/m_b$ is (Hui et al. 2017, see also Lora et al. (2012))

$$\mathbf{F}_f = -4\pi G^2 m_t^2 \rho_b \frac{\mathbf{v}_t - \mathbf{v}}{|\mathbf{v}_t - \mathbf{v}|^3} C(\beta, \gamma), \quad (66)$$

where $C(\beta, \gamma)$ is defined in Hui et al. (2017, equation D7) and

$$\beta = \frac{G m_b m_t}{\hbar |\mathbf{v}_t - \mathbf{v}|}, \quad \gamma = \frac{m_b b_{\max}}{\hbar} |\mathbf{v}_t - \mathbf{v}|. \quad (67)$$

Here, b_{\max} is some large radius around m_t , beyond which we assume that the gravitational force from the medium can be ignored. Integrating equation (66) over the DF $F_b(\mathbf{v})$, we obtain the rate of velocity drift due to dynamical friction,

$$D_f[\Delta v_i] = -4\pi G^2 m_t \int d\mathbf{v}' \frac{v_{t,i} - v'_i}{|\mathbf{v}_t - \mathbf{v}'|^3} F_b(\mathbf{v}') C\left(\frac{G m_b m_t}{\hbar |\mathbf{v}_t - \mathbf{v}'|}, \frac{m_b b_{\max}}{\hbar} |\mathbf{v}_t - \mathbf{v}'|\right). \quad (68)$$

To make an approximate estimate of the size of the quantities β and γ , we replace $|\mathbf{v}_t - \mathbf{v}'|$ by the velocity dispersion σ . Then,

$$\gamma \approx \frac{m_b b_{\max}}{\hbar} \sigma = \frac{b_{\max}}{\lambda_\sigma} = \frac{1}{2} \Lambda_{\text{FDM}} \quad (69)$$

where as usual $\lambda_\sigma = \hbar/(m_b \sigma)$ is the typical de Broglie angular wavelength, and Λ_{FDM} is the Coulomb factor defined in equation (2). Similarly,

$$\beta \simeq \frac{G m_b m_t}{\hbar \sigma} = \frac{b_{90}}{\lambda_\sigma}, \quad (70)$$

where $b_{90} = G m_t / \sigma^2$ is the 90° deflection radius. In the case $\beta \gg 1$, the de Broglie wavelength is negligible, and we recover the classical formula for dynamical friction (see Hui et al. 2017).

When $\beta \ll 1$ we use the result (Hui et al. 2017)

$$C(\beta, \gamma) = \mathbb{W}(\gamma) + \mathcal{O}(\beta), \quad (71)$$

where

$$\mathbb{W}(x) \equiv \text{Cin}(2x) + \frac{\sin(2x)}{2x} - 1, \quad (72)$$

and $\text{Cin}(x) \equiv \int_0^x (1 - \cos t) dt/t$ is a cosine integral. Our approximation of a homogeneous medium is only valid if the de Broglie wavelength is small compared to the system size, so $\gamma \gg 1$ and we can use the asymptotic expansion $\mathbb{W}(x) \rightarrow \log(2x) + \gamma_E - 1 + \mathcal{O}(1/x)$. Thus, $C(\beta, \gamma) \simeq \log \Lambda_{\text{FDM}} + [\log(|\mathbf{v}_t - \mathbf{v}'|/\sigma) + \gamma_E - 1]$. We may drop the term in square brackets, which is of order unity and hence small compared to the Coulomb logarithm, and write

$$\begin{aligned} D_f[\Delta v_i] &\simeq -4\pi G^2 m_t \log \Lambda_{\text{FDM}} \int d\mathbf{v}' \frac{v_i - v'_i}{|\mathbf{v} - \mathbf{v}'|^3} F_b(\mathbf{v}') \\ &= 4\pi G^2 m_t \log \Lambda_{\text{FDM}} \frac{\partial}{\partial v_i} \int d\mathbf{v}' \frac{1}{|\mathbf{v} - \mathbf{v}'|} F_b(\mathbf{v}'). \end{aligned} \quad (73)$$

Equation (73) is identical to the classical formula for dynamical friction (e.g., Tremaine & Weinberg 1984; Binney & Tremaine 2008) except that the Coulomb logarithm is defined by the ratio of the size of the system to the de Broglie wavelength, rather than to the 90° deflection radius (i.e., Λ_{cl} in eq. 2 is replaced by Λ_{FDM}). Moreover $D_f[\Delta v_i]$ is identical to the drift coefficient for a test particle $D_i = D[\Delta v_i]$ (eq. 24), except that the particle mass m_p is replaced by the massive body's mass m_t . For the Maxwellian velocity distribution (eq. 29), $D_f[\Delta v_i] = (v_i/v) D_f[\Delta v_{\parallel}]$, where

$$D_f[\Delta v_{\parallel}] = -\frac{4\pi G^2 \rho_b m_t \log \Lambda_{\text{FDM}}}{\sigma^2} \mathbb{G}(X), \quad (74)$$

with $\mathbb{G}(X)$ defined in equation (33).

4. MASS SEGREGATION

In most current CDM models, the dark matter consists of elementary particles whose mass is negligible compared to that of any astrophysical object. Even if the CDM particles are macroscopic objects, say of 1–30 M_\odot , they are much less massive than objects such as supermassive black holes or globular clusters. Therefore, these objects will inspiral toward the center of a CDM halo due to dynamical friction (e.g., Tremaine et al. 1975; Begelman et al. 1980). The situation is quite different in an FDM halo. As shown in earlier sections, FDM behaves as if it were composed of quasiparticles with an effective mass given by equation (64). Thus, although the massive object still loses orbital energy by dynamical friction, it can also gain energy by gravitational interactions with the quasiparticles. We expect that the inspiral of the massive object will stall if it reaches energy equipartition with the quasiparticles. For similar reasons, individual stars will tend to gain energy from interactions with the FDM quasiparticles, and this process can lead to the expansion of a stellar system embedded in the halo.

To explore these processes quantitatively, we use a simple model of a galaxy containing only FDM, with density ρ_b and a Maxwellian velocity distribution with dispersion σ (eq. 29). Then, we can combine equations (55)–(56) and (74) to obtain the diffusion coefficients for a point mass m_t ,

$$D[\Delta v_{\parallel}] = -\frac{4\pi G^2 \rho_b m_{\text{eff}} \log \Lambda_{\text{FDM}}}{\sigma_{\text{eff}}^2} [\mathbb{G}(X_{\text{eff}}) + \mu_{\text{eff}} \mathbb{G}(X)], \quad (75)$$

$$D[(\Delta v_{\parallel})^2] = \frac{4\sqrt{2}\pi G^2 \rho_b m_{\text{eff}} \log \Lambda_{\text{FDM}}}{\sigma_{\text{eff}}} \frac{\mathbb{G}(X_{\text{eff}})}{X_{\text{eff}}}, \quad (76)$$

$$D[(\Delta \mathbf{v}_{\perp})^2] = \frac{4\sqrt{2}\pi G^2 \rho_b m_{\text{eff}} \log \Lambda_{\text{FDM}}}{\sigma_{\text{eff}}} \frac{\text{erf}(X_{\text{eff}}) - \mathbb{G}(X_{\text{eff}})}{X_{\text{eff}}}, \quad (77)$$

where $\mathbb{G}(X)$ is defined in equation (33), $\sigma_{\text{eff}}^2/\sigma^2 = 1/2$, $X = v/\sqrt{2}\sigma$, $X_{\text{eff}} = v/\sqrt{2}\sigma_{\text{eff}} = v/\sigma$, and

$$\mu_{\text{eff}} \equiv \frac{m_t}{m_{\text{eff}}} \frac{\sigma_{\text{eff}}^2}{\sigma^2} = \frac{m_t}{2m_{\text{eff}}} \quad (78)$$

is the effective mass ratio. Note the factor of 2 in the definition of μ_{eff} , and note also that the classical diffusion coefficient analogous to equation (75) for a halo composed of particles of mass m_p is

$$D[\Delta v_{\parallel}] = -\frac{4\pi G^2 \rho_p m_p \log \Lambda_{\text{cl}}}{\sigma^2} (1 + \mu_{\text{cl}}) \mathbb{G}(X), \quad (79)$$

where $\mu_{\text{cl}} = m_t/m_p$ (without a factor of 2).

We stress again that the diffusion coefficients in equations (75)–(77) do not go to the classical ones in the limit $\hbar \rightarrow 0$ (or $m_{\text{eff}} \rightarrow 0$). This incompleteness is related to our simplifying assumption about the wave function in Section 2.2 (see discussion after eq. 48). In the Appendix A we extend the derivation of Section 2.2 to include the classical limit. There, we show that when $m_b \gg m_{\text{eff}}$, the relaxation becomes the classical one (i.e., as in a system of classical particles of mass m_b with velocity dispersion σ). This ‘‘classical’’ correction is negligible for the FDM mass considered here, $m_b < 10^{-20}$ eV, for which we can expect that the dynamics will deviate from the standard CDM case.

The specific energy diffusion coefficients are

$$\begin{aligned} D[\Delta E] &= vD[\Delta v_{\parallel}] + \frac{1}{2}D[(\Delta v_{\parallel})^2] + \frac{1}{2}D[(\Delta \mathbf{v}_{\perp})^2] \\ &= \frac{4\sqrt{2}\pi G^2 \rho_b m_{\text{eff}} \log \Lambda_{\text{FDM}}}{\sigma_{\text{eff}}} [\exp(-X_{\text{eff}}^2) - \mu_{\text{eff}} \sqrt{\pi} X_{\text{eff}} \mathbb{G}(X)] \\ &= \frac{8\sqrt{\pi} G^2 \rho_b m_{\text{eff}} \log \Lambda_{\text{FDM}}}{\sigma} \exp(-v^2/\sigma^2) [1 - \mu_{\text{eff}} K(v/\sigma)], \end{aligned} \quad (80)$$

and

$$D[(\Delta E)^2] = v^2 D[(\Delta v_{\parallel})^2] = 8\sqrt{2}\pi G^2 \rho_b m_{\text{eff}} \sigma_{\text{eff}} \log \Lambda_{\text{FDM}} X_{\text{eff}} \mathbb{G}(X_{\text{eff}}), \quad (81)$$

where we defined the dimensionless function

$$K(x) \equiv \frac{\sqrt{\pi}}{x} e^{x^2} \text{erf}(x/\sqrt{2}) - \sqrt{2} e^{x^2/2}. \quad (82)$$

The mean change in energy (eq. 80) arises from the competition between two processes: (i) diffusion (“heating”), a term resulting from the potential fluctuations of the FDM field that is proportional to m_{eff} and pumps energy into the orbit of the massive body, and (ii) dynamical friction (“cooling”), a term resulting from the back-reaction of the massive body on the FDM that is proportional to the body’s mass m_t and transfers energy from its orbit into the FDM field. The ratio between cooling and heating is given by $\mu_{\text{eff}}K(v/\sigma)$.

To investigate this process in more detail, let us consider an ensemble of systems, each containing a single body of mass m_t traveling in a uniform background of FDM. The velocities of these bodies are distributed according to a Maxwellian DF $F_t(\mathbf{v}_t)$, analogous to equation (29) but with density and velocity dispersion ρ_t and σ_t . The flow of specific energy into the orbits of the massive objects is

$$\begin{aligned} \langle \dot{E} \rangle &= \frac{1}{\rho_t} \int d\mathbf{v}_t F_t(\mathbf{v}_t) D[\Delta E] \\ &= \frac{8\sqrt{\pi}G^2 \rho_b m_{\text{eff}} \log \Lambda_{\text{FDM}}}{\sigma(1 + 2\sigma_t^2/\sigma^2)^{3/2}} \left[1 - \mu_{\text{eff}} \frac{\sqrt{2}\sigma_t^2}{\sigma^2} \frac{(1 + 2\sigma_t^2/\sigma^2)^{3/2}}{(1 + \sigma_t^2/\sigma^2)^{3/2}} \right]. \end{aligned} \quad (83)$$

When $m_t \ll m_{\text{eff}}$ or $\mu_{\text{eff}} \ll 1$, heating dominates, and we can use equation (83) to write

$$\frac{d\sigma_t^2}{dt} = \frac{2}{3} \langle \dot{E} \rangle = \frac{\sigma^2}{T_{\text{heat}}} (1 + 2\sigma_t^2/\sigma^2)^{-3/2}, \quad (84)$$

where we defined

$$T_{\text{heat}} = \frac{3\sigma^3}{16\sqrt{\pi}G^2 \rho_b m_{\text{eff}} \log \Lambda_{\text{FDM}}} = \frac{3m_b^3 \sigma^6}{16\pi^2 G^2 \rho_b^2 \hbar^3 \log \Lambda_{\text{FDM}}}, \quad (85)$$

as the heating timescale. The solution to equation (84) is

$$\frac{\sigma_t^2(t)}{\sigma^2} = \frac{1}{2} \left\{ 5t/T_{\text{heat}} + [1 + 2\sigma_t^2(0)/\sigma^2]^{5/2} \right\}^{2/5} - \frac{1}{2}. \quad (86)$$

Therefore, at time t , the velocity dispersion σ_t^2 should be at least $\frac{1}{2}(5t/T_{\text{heat}} + 1)^{2/5} - \frac{1}{2}$ times σ^2 , and σ_t will exceed σ in a time $t \lesssim 3T_{\text{heat}}$.

When $\mu_{\text{eff}} \gg 1$, cooling dominates, and equation (83) can be written as

$$\frac{d\sigma_t^2}{dt} = -\frac{\sigma_t^2}{T_{\text{cool}}} (1 + \sigma_t^2/\sigma^2)^{-3/2}, \quad (87)$$

in which we defined

$$T_{\text{cool}} = \frac{3\sigma^3}{8\sqrt{2\pi}G^2 m_t \rho_b \log \Lambda_{\text{FDM}}}, \quad (88)$$

as the cooling time. As expected, T_{cool} is independent of the effective mass of the FDM and is identical to the classical result except for a change in the Coulomb logarithm.

When T_{heat} and T_{cool} are smaller than the lifetime of the system, the distribution of velocities of the ensemble of massive objects will relax to a steady state, which is determined by requiring that its DF $F_t(\mathbf{v})$ satisfy the zero-flux condition in energy space:

$$\frac{d}{dv} \left\{ D[(\Delta E)^2] v F_t(v) \right\} = 2v^2 D[(\Delta E)] F_t(v). \quad (89)$$

This is solved to give

$$F_t(v) \propto \frac{1}{v D[(\Delta E)^2]} \exp \int_0^v dv' \frac{2v' D[(\Delta E)]}{D[(\Delta E)^2]}, \quad (90)$$

with the normalization chosen so that $\int d\mathbf{v} F_t(v) = \rho_t$.

As the diffusion coefficients depend linearly on the halo mass density ρ_b , the velocity distribution $F_t(v)$ depends on ρ_b only through μ_{eff} , via the dependence of the effective mass m_{eff} on ρ_b (eq. 59). For a classical N -body system composed of particles of mass m_p , $F_t(v)$ is a Maxwellian with mean-square velocity $3(m_p/m_t)\sigma^2$. In contrast, the steady-state velocity distribution of an ensemble of massive bodies interacting gravitationally with the FDM field is only approximately Maxwellian (see Figure 1), although the mean-square velocity is close to $3\sigma_{\text{eff}}^2/\mu_{\text{eff}} = 3(m_{\text{eff}}/m_t)\sigma^2$, similar to the classical relation (see Figure 2).

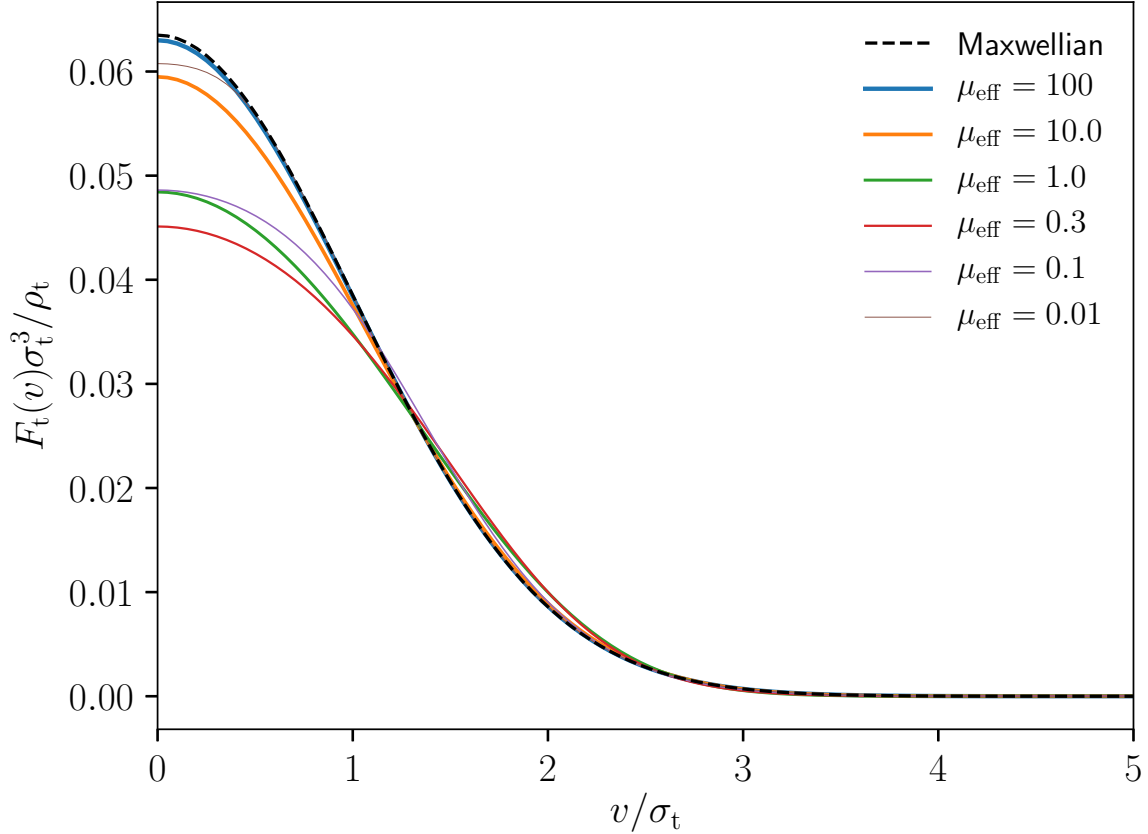


Figure 1. The steady-state velocity distribution for an ensemble of massive bodies interacting with an FDM field, as obtained from equation (90) for several values of the effective mass ratio $\mu_{\text{eff}} \equiv m_t/(2m_{\text{eff}})$ (solid lines). The velocity is plotted in units of the velocity dispersion, σ_t , where $\sigma_t^2 = \langle v^2 \rangle/3$. The steady-state velocity distribution approaches a Maxwellian (dashed line) in the limits $\mu_{\text{eff}} \rightarrow 0$ and $\mu_{\text{eff}} \rightarrow \infty$.

4.1. Examples

We now give two examples of the dynamical interaction between an FDM halo and baryonic objects orbiting within it. These examples are based on a simplified model of the FDM halo, consisting of two components:

The central soliton—Near the center, the FDM is condensed into a soliton, which is the ground-state solution of the Schrödinger–Poisson equations. The density of the soliton can be approximated by (Schive et al. 2014a)

$$\rho_s(r) \approx \frac{0.019 M_\odot \text{pc}^{-3}}{[1 + 0.091(r/r_s)^2]^8} \left(\frac{m_b}{10^{-22} \text{eV}} \right)^{-2} \left(\frac{r_s}{\text{kpc}} \right)^{-4}. \quad (91)$$

The total soliton mass is

$$M_s = 4\pi \int_0^\infty r^2 dr \rho_s(r) = 2.2 \times 10^8 M_\odot \left(\frac{r_s}{\text{kpc}} \right)^{-1} \left(\frac{m_b}{10^{-22} \text{eV}} \right)^{-2}. \quad (92)$$

Numerical simulations of the evolution of FDM halos in a cosmological context find that the soliton core radius r_s is related to the total halo (virial) mass M_h by (Schive et al. 2014b)

$$r_s \simeq 0.16 \text{ kpc} \left(\frac{m_b}{10^{-22} \text{eV}} \right)^{-1} \left(\frac{M_h}{10^{12} M_\odot} \right)^{-1/3}, \quad (93)$$

The relation between halo mass and peak circular speed v_{max} outside the soliton is the same as in CDM (Klypin et al. 2011),

$$v_{\text{max}} = 155 \text{ km s}^{-1} \left(\frac{M_h}{10^{12} M_\odot} \right)^{0.316}, \quad (94)$$

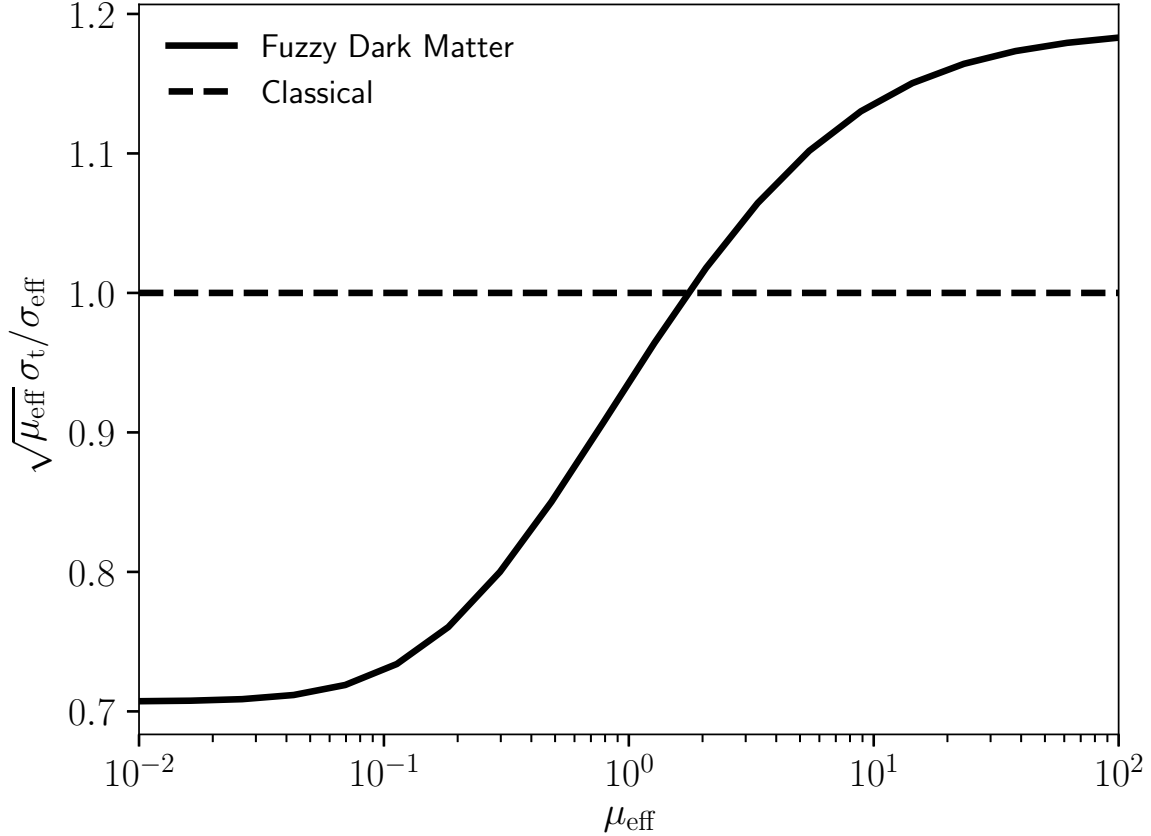


Figure 2. In thermal equilibrium, the velocity dispersion σ_t of an ensemble of baryons is related to the effective velocity dispersion $\sigma_{\text{eff}} = \sigma/\sqrt{2}$ of the FDM halo. The ratio of dispersions depends on the effective mass ratio $\mu_{\text{eff}} \equiv m_t/(2m_{\text{eff}})$ (solid line) and is close to (within 30%) but not equal to the standard relation $\sqrt{m_t/m_p} \sigma_t/\sigma = 1$ (dashed line) that corresponds to the thermal equilibrium in a background of classical particles of mass m_p and velocity dispersion σ .

so the relation between the soliton core radius and the peak circular speed is

$$r_s \simeq 0.12 \text{ kpc} \left(\frac{m_b}{10^{-22} \text{ eV}} \right)^{-1} \left(\frac{v_{\text{max}}}{200 \text{ km s}^{-1}} \right)^{-1.05}. \quad (95)$$

It is instructive to compare the typical de Broglie wavelength in the galaxy to the radius of the soliton, and we can do this in two ways. (i) The wavelength for a particle traveling at the circular speed at a distance r outside the soliton is given by the simple formula

$$\lambda = \frac{h}{m_b} \left(\frac{r}{GM_s} \right)^{1/2} = 3.91 r_s \left(\frac{r}{r_s} \right)^{1/2}. \quad (96)$$

In other words, the de Broglie wavelength just outside the soliton is on the order the soliton radius. (ii) The de Broglie wavelength for a particle traveling at the peak circular speed is

$$\lambda = \frac{h}{m_b v_{\text{max}}} = 0.60 \text{ kpc} \left(\frac{m_b}{10^{-22} \text{ eV}} \right)^{-1} \left(\frac{v_{\text{max}}}{200 \text{ km s}^{-1}} \right)^{-1}. \quad (97)$$

Once again, the de Broglie wavelength is a few times the soliton radius (eq. 95). The agreement between methods (i) and (ii) reflects the fact that the empirical relation (93) implies that the peak circular speed in the soliton is almost the same (25% smaller) as the peak circular speed in the halo, independent of the particle mass and almost independent of the halo mass. This coincidence is an unexplained feature of the evolution of FDM halos.

The halo—Outside the soliton, the mean FDM density distribution is expected to be similar to that of CDM halos, which can be fit empirically by the Navarro et al. (1997) profile. We shall adopt an even simpler model, in which outside the soliton, the FDM density is given by a singular isothermal sphere (eq. 63). The effective mass (eq. 59) of the FDM field at radius $r \gg r_s$ is then given by equation (64), and the typical de Broglie wavelength is given by equation (65).

4.1.1. Inspiral of a massive object

An object of mass m_t on a circular orbit of initial radius r_i will inspiral toward the central soliton if the effective mass ratio $\mu_{\text{eff}} \gg 1$ (eq. 80). The inspiral time is (Binney & Tremaine 2008, eq. 8.12)

$$\begin{aligned} t_{\text{inspiral}} &= \frac{1.65 r_i^2 \sigma}{\log \Lambda_{\text{FDM}} G m_t} \\ &= \frac{84.9 \text{ Gyr}}{\log \Lambda_{\text{FDM}}} \frac{10^7 M_\odot}{m_t} \frac{v_c}{200 \text{ km s}^{-1}} \left(\frac{r_i}{4 \text{ kpc}} \right)^2. \end{aligned} \quad (98)$$

The object will spiral to the center in less than the age of the galaxy, T_{age} , if

$$r_i < 2.08 \text{ kpc} \left(\frac{\log \Lambda_{\text{FDM}}}{\log 10} \frac{m_t}{10^7 M_\odot} \frac{T_{\text{age}}}{10 \text{ Gyr}} \frac{200 \text{ km s}^{-1}}{v_c} \right)^{1/2}. \quad (99)$$

However, as the radius of the orbit shrinks, the effective mass grows as r^{-2} (eq. 64), so $\mu_{\text{eff}} \propto r^2$. The effective mass ratio is less than unity inside a stalling radius

$$r_{\text{stall}} = (2\pi)^{1/4} \left(\frac{\hbar^3}{G m_t m_b^3 v_c} \right)^{1/2} = 1.43 \text{ kpc} \left(\frac{m_t}{10^7 M_\odot} \right)^{-1/2} \left(\frac{m_b}{10^{-22} \text{ eV}} \right)^{-3/2} \left(\frac{v_c}{200 \text{ km s}^{-1}} \right)^{-1/2}. \quad (100)$$

In early-type galaxies (ellipticals and spiral bulges), the mass of the central black hole is correlated with the velocity dispersion (Kormendy & Ho 2013),

$$\log_{10} \frac{M_\bullet}{10^9 M_\odot} = -0.51 \pm 0.05 + (4.4 \pm 0.3) \log_{10} \frac{\sigma}{200 \text{ km s}^{-1}} \quad (101)$$

with a scatter of about 0.3 dex. If we assume that the circular speed and dispersion are related by $\sigma = v_c / \sqrt{2}$ as in the isothermal sphere, and that the mass of the inspiraling black hole is $m_t = f M_\bullet$ with $f < 1$, then these relations can be rewritten as

$$r_i < 3.1 \text{ kpc} \left(\frac{f}{0.1} \frac{\log \Lambda_{\text{FDM}}}{\log 10} \frac{T_{\text{age}}}{10 \text{ Gyr}} \right)^{1/2} \left(\frac{\sigma}{200 \text{ km s}^{-1}} \right)^{1.7}; \quad (102)$$

$$r_{\text{stall}} = 0.70 \text{ kpc} \left(\frac{f}{0.1} \right)^{-1/2} \left(\frac{m_b}{10^{-22} \text{ eV}} \right)^{-3/2} \left(\frac{\sigma}{200 \text{ km s}^{-1}} \right)^{-2.7}. \quad (103)$$

These results suggest that the inspiral of supermassive black holes in FDM halos may be stalled at orbital radii of a few hundred parsecs, a possibility that has been discussed already by Hui et al. (2017). Although we believe that the physical mechanism described here is robust, there are two (related) shortcomings in these calculations: (i) for the parameters of interest, the stalling radius can be comparable to or even smaller than the typical de Broglie radius λ_σ (eq. 65); because the maximum scale of the encounters for which our approximations are valid is then $b_{\text{max}} \simeq r_{\text{stall}}$, the argument of the Coulomb logarithm is $\Lambda_{\text{FDM}} = 2r_{\text{stall}}/\lambda_\sigma$ (eq. 61), small enough that the assumption $\Lambda_{\text{FDM}} \gg 1$ on which our calculations are based is suspect; (ii) the stalling radius is not much larger than the core radius of the central soliton r_s (eq. 93), and inside the soliton, heating by fluctuations in the FDM vanishes⁸ although dynamical friction does not. These limitations are related because the de Broglie wavelength just outside the soliton is of order the soliton radius (eqs. 96 and 97).

In Figure 3, we illustrate how energy diffusion due to scattering by FDM quasiparticles tampers with the otherwise deterministic inspiral due to dynamical friction. We followed the orbit of a massive object ($m_t = 4 \times 10^5 M_\odot$) in a singular isothermal sphere

⁸ This conclusion assumes that the soliton is in its ground state. Simulations by Veltmaat et al. (2018) suggest that the soliton typically exhibits strong density oscillations, which could add energy to nearby orbits.

(eq. 63) having circular speed $v_c = 200 \text{ km s}^{-1}$, and applied random velocity changes using the diffusion coefficients (75)–(77) with $m_b = 10^{-21} \text{ eV}$. We repeated this process 1000 times, and Figure 3 shows the median and 68% confidence band of the orbital radius as a function of time. For comparison, we also applied (deterministic) velocity changes due to dynamical friction only (eq. 74) both for FDM and CDM halos, which differ only in the Coulomb logarithm. The results shown in Figure 3 are consistent with our claim that a massive object that is inspiraling to the center by dynamical friction will tend to stall, on average, at a radius where the effective mass ratio $\mu_{\text{eff}} \simeq 1$.

In Figure 4, we show the relation between the maximum inspiral distance r_i (eq. 99), the stalling radius r_{stall} (eq. 100), and the typical de Broglie wavelength λ_σ (eq. 65) of a galaxy with circular speed $v_c = 200 \text{ km s}^{-1}$, for a range of massive objects and FDM particle masses. Similarly, in Figure 5, we show the relation between the maximum inspiral distance r_i (eq. 102), the stalling radius r_{stall} (eq. 103), and the typical de Broglie wavelength λ_σ (eq. 65) for a massive object that is a fraction $f = 0.1$ of the central black hole mass inferred from the M – σ relation (eq. 101) for galaxies with a range of velocity dispersions and FDM particle masses.

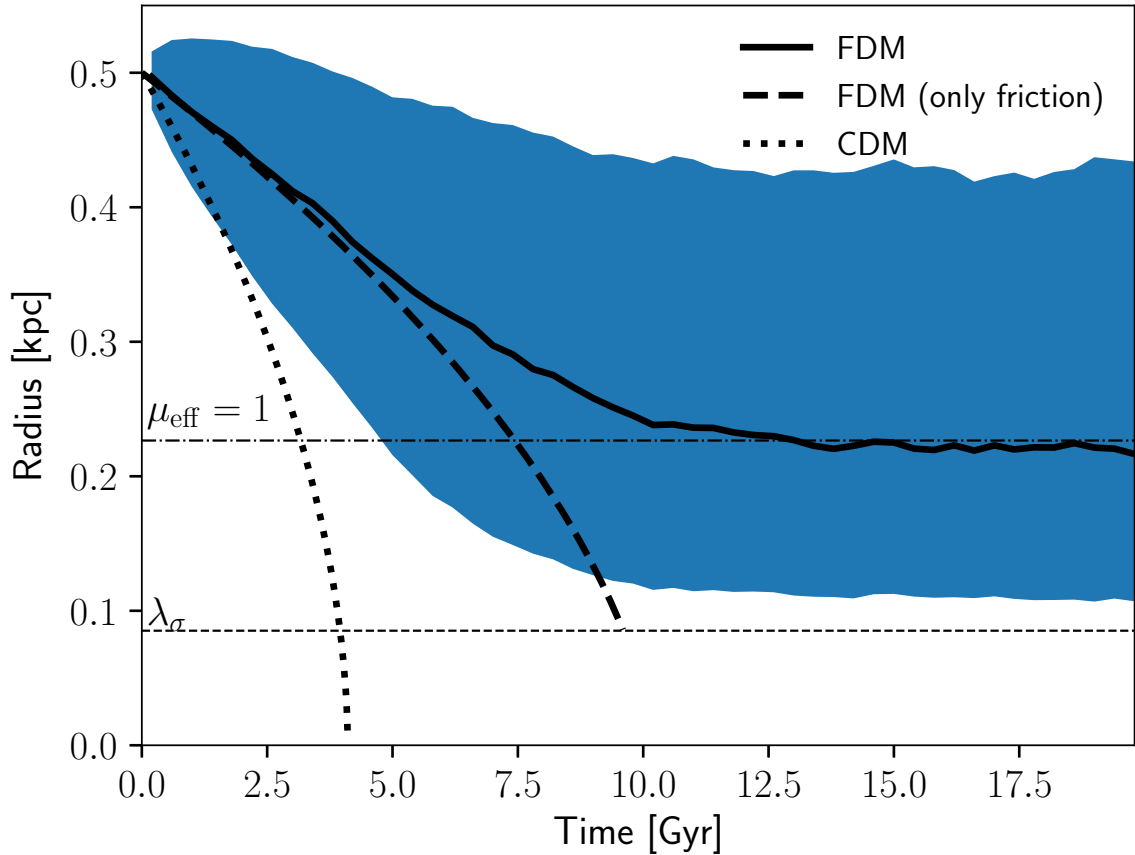


Figure 3. The inspiral of a massive object ($m_t = 4 \times 10^5 M_\odot$) on a circular orbit in a spherical galaxy with constant circular speed $v_c = 200 \text{ km s}^{-1}$ (eq. 63). The dotted line shows the evolution of the orbital radius due to dynamical friction if the galaxy is composed of CDM (eq. 79 with $\mu_{\text{cl}} \gg 1$). The dashed line shows the evolution due to dynamical friction if the galaxy is composed of FDM (eq. 74) and diffusion terms are ignored. This differs from the CDM case only through the Coulomb logarithm. The solid line and shaded region show the evolution in an FDM galaxy including both dynamical friction and diffusion, assuming an FDM mass $m_b = 10^{-21} \text{ eV}$. We have carried out 1000 realizations of the orbital evolution, and the solid line and shaded region show the median and central 68% region. The median radius saturates close to where $\mu_{\text{eff}} = 1$ (dashed-dotted horizontal line). This behavior is different from the case where diffusion is ignored (dashed line), for which dynamical friction causes the orbit to decay at least down to the de Broglie wavelength λ_σ (dashed horizontal line).

4.1.2. Heating of a spherical stellar population

We consider the effect of FDM fluctuations on a stellar system having a Maxwellian DF with velocity dispersion σ_t . We assume that the gravitational potential is dominated by FDM and that the typical radius of the stellar system is r_* . Since m_{eff} is

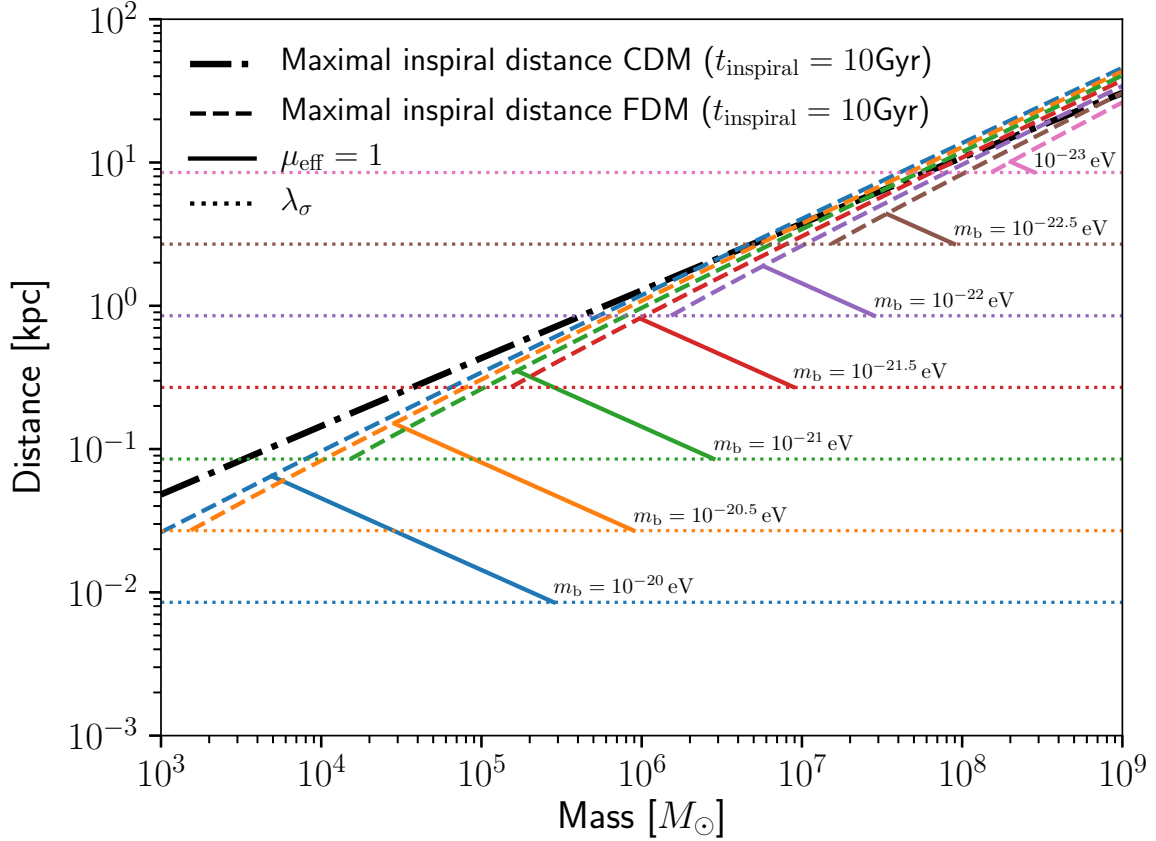


Figure 4. A massive object initially on a circular orbit will spiral to the center within 10 Gyr if it lies below the dashed lines (eq. 99). Different colors represent different assumptions about the mass of the FDM particle, and the heavy dashed-dotted black line shows the same curve for CDM. The solid lines show the radius r_{stall} (eq. 100) where stochastic potential fluctuations cause the inspiral to stall. The solid lines terminate when the stalling radius is smaller than the typical de Broglie wavelength λ_σ (dotted lines); at smaller distances, the evolution is dominated by interactions with the soliton, which exerts dynamical friction but has no potential fluctuations. We assume that the density of the FDM is that of a singular isothermal sphere (eq. 63) with circular speed $v_c = 200 \text{ km s}^{-1}$.

much larger than the mass of any individual star, dynamical friction and cooling are negligible. The heating timescale is given by equations (85) and (63):

$$T_{\text{heat}} = \frac{3m_b^3 v_c^2 r_\star^4}{8h^3 \log \Lambda_{\text{FDM}}} \approx \frac{2.08 \text{ Gyr}}{\log \Lambda_{\text{FDM}}} \left(\frac{r_\star}{1 \text{ kpc}} \right)^4 \left(\frac{m_b}{10^{-22} \text{ eV}} \right)^3 \left(\frac{v_c}{200 \text{ km s}^{-1}} \right)^2. \quad (104)$$

The heating will be significant if T_{heat} is less than a third of the age of the galaxy T_{age} (see discussion following eq. 86), which occurs if $r_\star < r_{\text{heat}}$ where the heating radius is

$$r_{\text{heat}} = 1.13 \text{ kpc} \left(\log \Lambda_{\text{FDM}} \frac{T_{\text{age}}}{10 \text{ Gyr}} \right)^{1/4} \left(\frac{v_c}{200 \text{ km s}^{-1}} \right)^{-1/2} \left(\frac{m_b}{10^{-22} \text{ eV}} \right)^{-3/4}. \quad (105)$$

The approximations we are using are only valid if the orbital radius is significantly larger than the de Broglie wavelength. Setting $r_\star = \lambda_\sigma$ we obtain a minimum heating time

$$T_{\text{heat}}^{\text{min}} = \frac{24\pi^4 \hbar}{m_b v_c^2 \log \Lambda_{\text{FDM}}} \approx 0.43 \text{ Gyr} \left(\frac{m_b}{10^{-22} \text{ eV}} \right)^{-1} \left(\frac{v_c}{200 \text{ km s}^{-1}} \right)^{-2}. \quad (106)$$

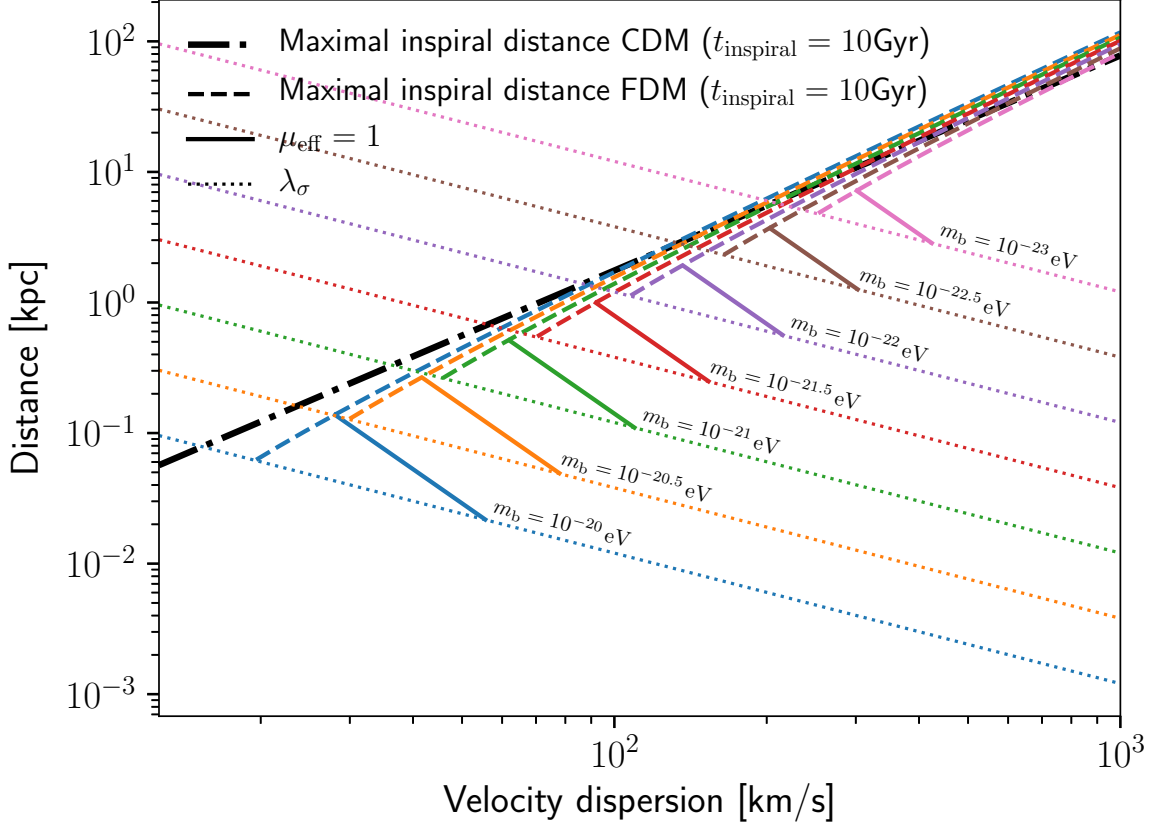


Figure 5. Same as Figure 4, except that the horizontal axis is the velocity dispersion of the host galaxy and the mass of the inspiraling object is a fraction $f = 0.1$ of the mass of the central black hole inferred from the $M - \sigma$ relation (eq. 101).

In this result, we have evaluated the Coulomb logarithm at $b_{\max} = \lambda_{\sigma}$; thus, $\log \Lambda_{\text{FDM}} = \log 2b_{\max}/\lambda_{\sigma} = \log(4\pi) \approx 2.5$.

We remark that the term “heating” is misleading: the interaction with FDM fluctuations adds energy to the stellar population, thereby causing it to expand, but the velocity dispersion of the stars may either grow or decay as a result of this expansion depending on the radial profile of the gravitational potential of the galaxy. To illustrate this process, we followed the evolution of a population of test particles representing stars in an isothermal density distribution (eq. 63). The self-consistent gravitational potential of this distribution is $\Phi(r) = v_c^2 \log r$, which we modified to $\Phi(r) = \frac{1}{2}v_c^2 \log(r^2 + r_0^2)$ for reasons given below. The initial velocities of the test particles were drawn from an isotropic Maxwellian distribution with velocity dispersion σ_t and the initial positions were drawn from the radial distribution $dn \propto r^2(r_0^2 + r^2)^{-v_c^2/(2\sigma_t^2)} dr$, which ensures that the initial phase-space distribution is a stationary solution of the collisionless Boltzmann equation. We introduced a core radius r_0 into the potential, so the integral over the radial distribution remains convergent when $\sigma_t^2 \leq 3v_c^2$. The actual value of r_0 is unimportant since we set $r_0 = 0.2\lambda_{\sigma}$ and turned off the diffusion coefficients when $r < \lambda_{\sigma}$. We used the diffusion coefficients from equations (75)–(77).

In Figure 6 we show the evolution in an FDM halo having $v_c = 200 \text{ km s}^{-1}$ and $m_b = 10^{-21} \text{ eV}$. This figure shows the expansion (upper panels) and heating (lower panels) of a system of 5600 test particles with initial velocity dispersion $\sigma_t = v_c/2$ (left panels) and $\sigma_t = v_c/\sqrt{2}$ (right panels). In both cases, within a few Gyr, the velocity dispersion of the test particles exceeds that of the FDM (dashed horizontal lines), and the stellar density develops a core in the region outside the de Broglie wavelength and inside the radius where T_{heat} equals the age (shaded regions). Our assumption that fluctuations in the FDM density have no effect inside the de Broglie wavelength λ_{σ} is oversimplifying, so the sharp changes in density and dispersion at λ_{σ} are unrealistic.

In Figure 7, we show the heated region as a function of the circular speed for several values of the particle mass m_b , along with the effective radii and maximum circular speeds for the ATLAS^{3D} sample of elliptical galaxies (Cappellari et al. 2013a). These galaxies are most sensitive to particle masses in the range $m_b \sim 10^{-22}$ – 10^{-23} eV , which is somewhat smaller than the mass range of interest for influencing small-scale structure. To probe larger masses we need to look for evidence of heating at smaller

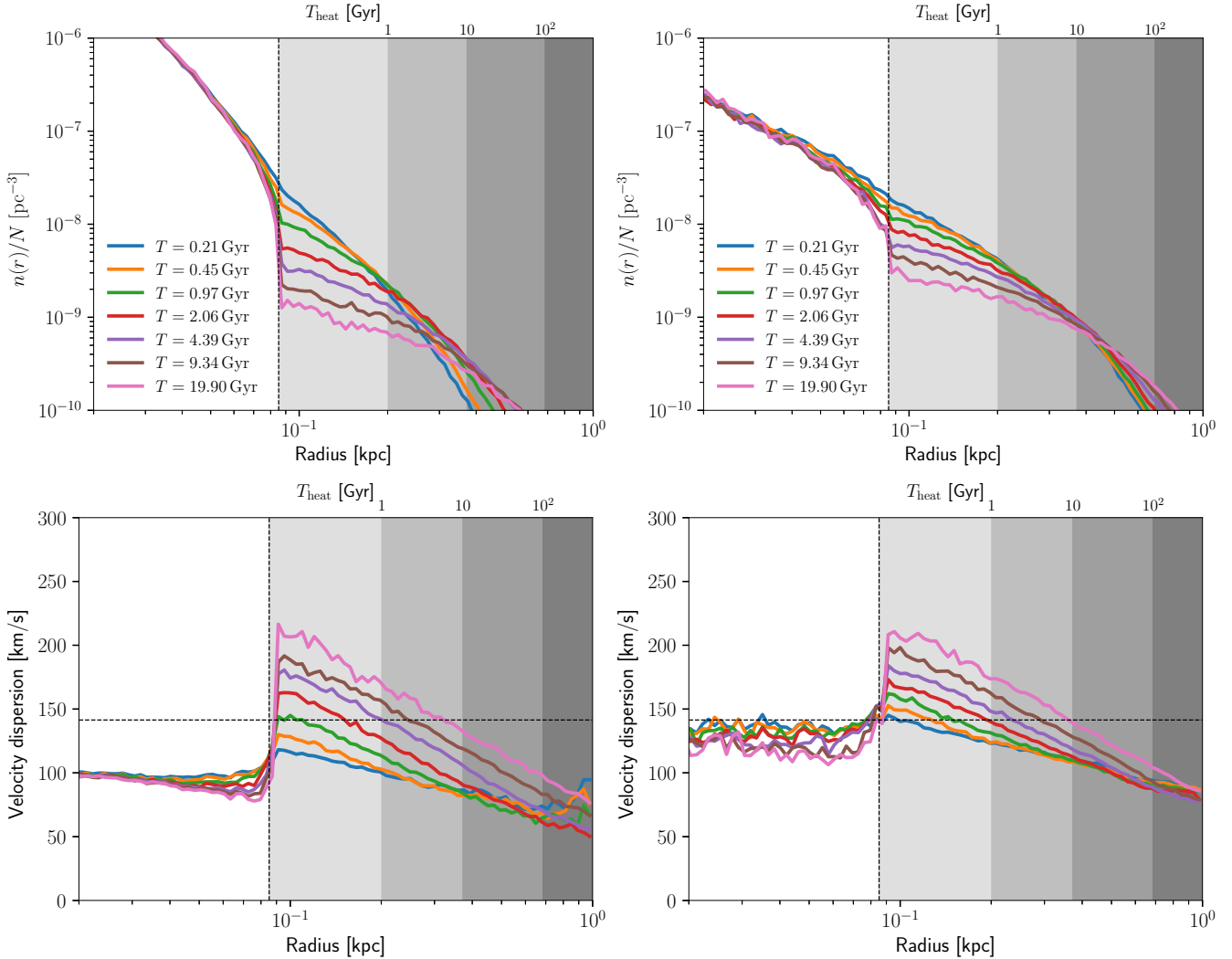


Figure 6. The expansion of a system of test particles in an isothermal FDM halo with particle mass $m_b = 10^{-21}$ eV and circular speed $v_c = 200$ km s $^{-1}$. The velocity dispersion $\sigma = v_c/\sqrt{2} \simeq 141$ km s $^{-1}$ (dashed horizontal lines). The test-particle distribution is initially isothermal with velocity dispersion $\sigma_\epsilon = v_c/2 = 100$ km s $^{-1}$ (left panels) and $v_c/\sqrt{2} \approx 141$ km s $^{-1}$ (right panels). In the region outside the de Broglie wavelength λ_s (dashed vertical lines), where the heating time is less than the age (top axis and shaded regions), the number density decreases (upper panels) and the velocity dispersion increases (bottom panels) as a function of time.

radii, but here, (i) most galaxies are not dark-matter dominated, and (ii) the FDM may be in the form of a ground-state soliton and thus would not heat the stars.

5. SUMMARY AND CONCLUSIONS

Fuzzy dark matter (FDM) is an intriguing alternative to CDM that may resolve some or all of the failures of CDM to predict the properties of the structure of galaxies on scales less than 30 kpc or so. FDM exhibits a rich set of novel phenomena. In particular, the density and gravitational potential fluctuations in an isolated CDM halo gradually decay as sub-halos are destroyed and tidal tails are phase-mixed. In contrast, an isolated FDM halo exhibits persistent density fluctuations that arise because of the limited number of eigenstates that it contains.

A test particle moving through the fluctuating FDM potential is subject to stochastic velocity changes. We calculated the diffusion coefficients that govern its resulting orbital evolution. For a Maxwellian velocity distribution with dispersion σ , these diffusion coefficients are the same as the diffusion coefficients in a classical N -body system if (i) the classical system is assumed to be composed of quasiparticles with an effective mass m_{eff} that depends on the local density (eq. 59); and (ii) the velocity dispersion of the quasiparticles is taken to be $\sigma/\sqrt{2}$; (iii) the lower limit of the range of scales in the classical Coulomb logarithm,

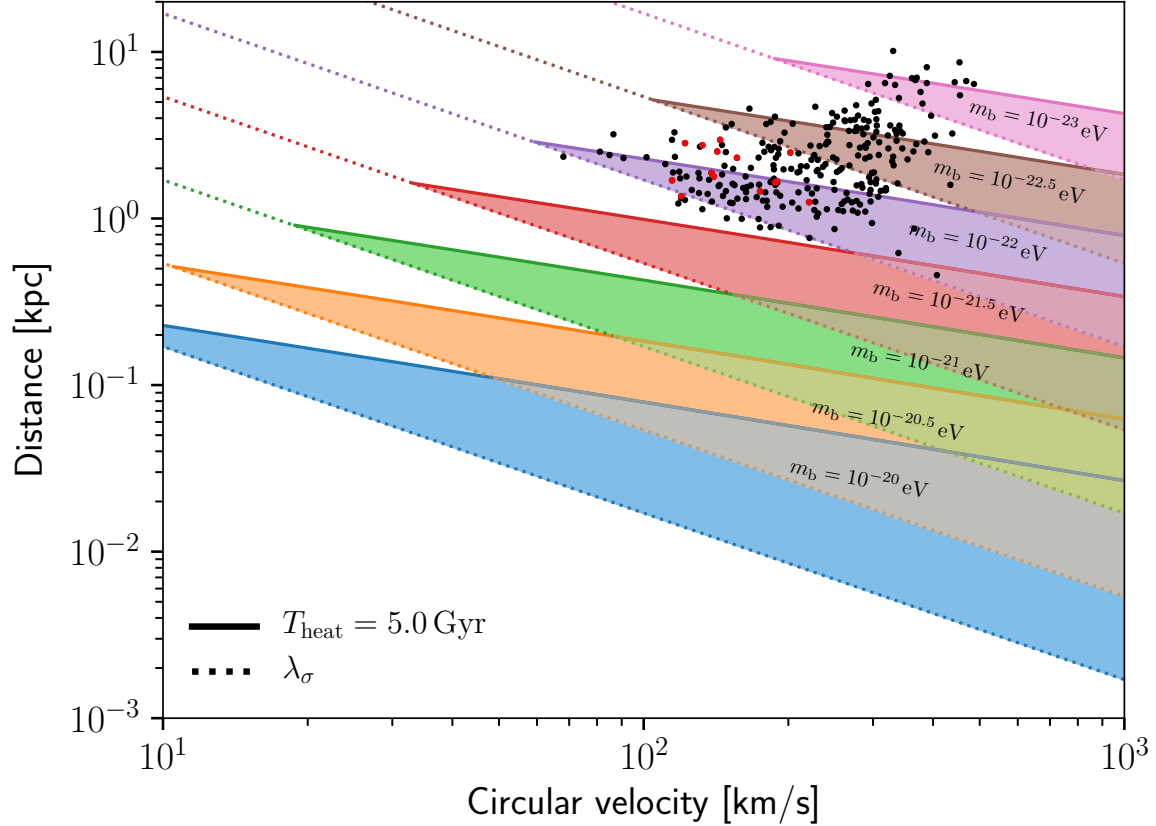


Figure 7. The heated region, in which $T_{\text{heat}} \leq 5$ Gyr (solid lines, eq. 104) and $r > \lambda_\sigma$ (dashed lines), for several values of the boson mass m_b . In the colored regions, old stellar systems will be heated significantly, causing the stellar system to expand and its velocity dispersion to grow (see Figure 6). For comparison, we show as circles the projected half-light radius and maximum circular speed v_c^{max} (circles) for the ATLAS^{3D} sample of 260 early-type galaxies (Cappellari et al. 2013a). The effects of FDM heating are overestimated in most of these because they are not dark-matter dominated near their centers; however, the 14 galaxies marked in red are estimated to have a dark-matter fraction larger than 0.5 (Cappellari et al. 2013b).

usually taken to be b_{90} , the impact parameter for a 90° deflection, is replaced by $\lambda_\sigma/2$, half of the typical de Broglie angular wavelength of the FDM. Similarly, the dynamical friction force on a massive particle orbiting in an FDM halo is given by the classical formula except that the Coulomb logarithm is modified as described in (iii).

In this paper, we assumed that the mean potential is infinite and homogeneous. In the classical case, this assumption implies that the unperturbed particles travel on straight lines at constant velocity, while in an FDM halo, it implies that the unperturbed wavefunction is a collection of plane waves of constant wavenumber and frequency. This is a standard simplification that is usually reasonably accurate when the Coulomb logarithm is much larger than unity, which in turn occurs when the radial scale is much larger than the typical wavelength. Unfortunately, the effects of FDM scattering on stellar systems are typically strongest at radii that are comparable to the wavelength. In such cases, the present derivation is incomplete, and further numerical and theoretical studies are needed. Nevertheless, we believe that our main conclusions are not seriously compromised by this limitation.

We showed that a massive object that is spiraling into the center of the galaxy by dynamical friction is subject to stochastic velocity fluctuations when it reaches a radius where its mass is comparable to the effective mass of the FDM quasiparticles. As this point, the FDM fluctuations pump energy into the orbit at roughly the same rate that it is drained by dynamical friction, so the inspiral will tend to stall.

Stars, which are much lighter than the FDM quasiparticles, will on average gain energy from the FDM fluctuations in the region where the relaxation time is much smaller than the age of the galaxy. Thus, stellar systems on scales of a few hundred pc to a few kpc will expand, and the heating time within the stellar system will be comparable to its lifetime. Therefore, one should not observe systems in which the heating time is much shorter than the age of the galaxy.

At the present, time neither of these physical processes offers a robust new constraint on the mass range of possible FDM particles. Other effects of relaxation due to FDM are discussed by [Hui et al. \(2017\)](#).

Finally, in this paper, we have discussed only the effects of FDM fluctuations on the orbits of classical objects such as stars and black holes. The effects of FDM fluctuations on the FDM halo itself are also important, but these must be analyzed using other tools (e.g., [Levkov et al. 2018](#); [Mocz et al. 2018](#)).

We thank Philip Mocz for thoughtful comments on an earlier version of this manuscript. BB acknowledges support from the Schmidt Fellowship. JBF acknowledges support from Program number HST-HF2-51374 which was provided by NASA through a grant from the Space Telescope Science Institute, which is operated by the Association of Universities for Research in Astronomy, Incorporated, under NASA contract NAS5-26555.

APPENDIX

A. THE CLASSICAL LIMIT OF FUZZY DARK MATTER

In our derivations in Section 2.2, we assumed that each plane wave has a random phase and is moving with velocity $\mathbf{v} = \hbar\mathbf{k}/m_b$. These assumptions are valid if the number of particles per wave $N \sim \rho_b \lambda^3 / m_b \sim \rho_b \hbar^3 / (\sigma^3 m_b^4)$ is large. Thus, our assumptions are valid when

$$m_b \ll m_s \equiv \left(\frac{\rho_b \hbar^3}{\sigma^3} \right)^{1/4} = \left(\frac{\hbar^3}{2\pi G \sigma r^2} \right)^{1/4} \simeq 35 \text{ eV} \left(\frac{r}{1 \text{ kpc}} \right)^{-1/2} \left(\frac{\sigma}{200 \text{ km s}^{-1}} \right)^{-1/4}, \quad (\text{A1})$$

in which we have used equation (63). From equation (59), we can see that the condition $m_b \ll m_s$ is equivalent to $m_b \ll m_{\text{eff}}$, that is, each quasiparticle of mass m_{eff} must contain many FDM particles of mass m_b .

At even larger masses, the system will behave like a classical system of free particles of mass m_b . Consider a free particle at position $x \pm \Delta x_0$ and velocity $v \pm \Delta v_0$, where Δx_0 and Δv_0 are the initial uncertainties in position and velocity, and $\Delta x_0 \Delta v_0 \geq \hbar/(2m_b)$. After a time T , the uncertainty in position is $\Delta x = \Delta x_0 + \Delta v_0 T \geq \Delta x_0 (1 + \hbar T / [2m_b (\Delta x_0)^2])$. The slowest scattering events have $T \simeq T_d$ where $T_d = r/\sigma$ is the dynamical time and r is the orbit radius. If the particles are to behave classically, the position uncertainty cannot grow significantly during the scattering and cannot exceed the typical distance between particles $d = (m_b/\rho_b)^{1/3}$, demanding that $d \gg \Delta x_0 \gg (\hbar T_d / 2m_b)^{1/2}$. Therefore, we can define a critical particle mass m_c at which $d = (\hbar T_d / 2m_b)^{1/2}$, and the particles behave classically if

$$m_b \gg m_c \equiv \rho_b^{2/5} (\hbar T_d / 2)^{3/5} = \frac{1}{2} \left(\frac{\hbar^3 \sigma}{\pi^2 G^2 r} \right)^{1/5} = 1.25 \times 10^{16} \text{ eV} \left(\frac{r}{1 \text{ kpc}} \right)^{-1/5} \left(\frac{\sigma}{200 \text{ km s}^{-1}} \right)^{1/5}. \quad (\text{A2})$$

Thus, there is an intermediate range $m_s \lesssim m_b \lesssim m_c$ in which the behavior needs further investigation, which we now undertake.

To make these arguments more quantitative we consider the following wave function:

$$\psi(\mathbf{r}, t) = \int d\mathbf{k} \varphi(\mathbf{k}) e^{i\mathbf{k}\cdot\mathbf{r} - i\omega(\mathbf{k})t}, \quad (\text{A3})$$

where $\omega(k)$ is given by equation (46), and the wave function in \mathbf{k} -space is a sum of Gaussian wavepackets,

$$\varphi(\mathbf{k}) = \sum_{n=1}^N \frac{\varepsilon^{3/2} m_b^{1/2}}{2^{3/4} \pi^{9/4}} e^{-|\mathbf{k} - m_b \mathbf{v}_n / \hbar|^2 \varepsilon^2} e^{i\phi_n - i\mathbf{k}\cdot\mathbf{r}_n}. \quad (\text{A4})$$

Here $\{\mathbf{r}_n\}$, $\{\mathbf{v}_n\}$ are random positions and velocities drawn from the DF $F_b(\mathbf{v})$, $\{\phi_n\}$ are independent random phases, and ε is the initial uncertainty in position. The normalization is such that $\langle |\psi|^2 \rangle = \rho_b$.

The correlation function of $\varphi(\mathbf{k})$ is given by $\langle \varphi(\mathbf{k}) \varphi^*(\mathbf{k}') \rangle = f_k(\mathbf{k}) \delta(\mathbf{k} - \mathbf{k}')$, where

$$f_k(\mathbf{k}) = \frac{8\varepsilon^3}{(2\pi)^{3/2}} \int d\mathbf{v} F_b(\mathbf{v}) e^{-2\varepsilon^2 |\mathbf{k} - m_b \mathbf{v} / \hbar|^2}, \quad (\text{A5})$$

and as expected the mean density is stationary, $\rho_b = \langle |\psi(\mathbf{r}, t)|^2 \rangle = \int d\mathbf{k} f_k(\mathbf{k}) = \int d\mathbf{v} F_b(\mathbf{v})$.

Assuming $F_b(\mathbf{v})$ is a Maxwellian DF with velocity dispersion σ , the correlation function for the density fluctuations $\rho(\mathbf{r}, t) = |\psi(\mathbf{r}, t)|^2 - \rho_b$ is

$$\begin{aligned} \langle \rho(\mathbf{r}, t) \rho(\mathbf{r}', t') \rangle = & \frac{\rho_b^2}{\left[1 + (1 + \alpha_1^2)^2 (\sigma \Delta t / \lambda_\sigma)^2\right]^{3/2}} \exp \left[-\frac{(|\Delta \mathbf{r}| / \lambda_\sigma)^2 (1 + \alpha_1^2)}{1 + (1 + \alpha_1^2)^2 (\sigma \Delta t / \lambda_\sigma)^2} \right] \\ & + \frac{m_b \rho_b}{8\pi^{3/2} \varepsilon^3 \left[1 + (\sigma \Delta t / \sqrt{2} \varepsilon)^2 + \alpha_2^2 / 2\right]^{3/2}} \exp \left[-\frac{(|\Delta \mathbf{r}| / 2\varepsilon)^2}{1 + (\sigma \Delta t / \sqrt{2} \varepsilon)^2 + \alpha_2^2 / 2} \right]. \end{aligned} \quad (\text{A6})$$

Here we have defined $\Delta \mathbf{r} = \mathbf{r} - \mathbf{r}'$, $\Delta t = t - t'$, $T = \sqrt{t^2 + t'^2}$, and two dimensionless parameters $\alpha_1 = \lambda_\sigma / (2\varepsilon)$ and $\alpha_2 = \hbar T / (2m_b \varepsilon^2)$.

Since we require the correlations to be stationary over a dynamical time $T_d \sim r/\sigma$, we can set $\varepsilon^2 \gg \lambda_\sigma r \gg \lambda_\sigma^2$ so $\alpha_1 \ll 1$. Moreover, when $T \lesssim T_d$, we have $\alpha_2 < \hbar T_d / (2m_b \varepsilon^2) \sim \lambda_\sigma r / \varepsilon^2 \ll 1$. Then, equation (A6) becomes

$$C(\mathbf{r}, t) = \frac{\rho_b^2}{\left[1 + (\sigma t / \lambda_\sigma)^2\right]^{3/2}} \exp \left[-\frac{(r / \lambda_\sigma)^2}{1 + (\sigma t / \lambda_\sigma)^2} \right] + \frac{m_b \rho_b}{8\pi^{3/2} \varepsilon^3 \left[1 + (\sigma t / \sqrt{2} \varepsilon)^2\right]^{3/2}} \exp \left[-\frac{(r / 2\varepsilon)^2}{1 + (\sigma t / \sqrt{2} \varepsilon)^2} \right]. \quad (\text{A7})$$

By comparing this result to the correlation function we obtained for FDM (eq. 62) and for classical particles (eq. 41), we can see that it is the sum of the FDM (first term) and the classical (second term) limits. The diffusion coefficients for a zero-mass test particle are now (cf. eqs. 75–77 and 30–32)

$$D[\Delta v_{\parallel}] = -4\pi G^2 \rho_b \left[\frac{m_{\text{eff}} \log \Lambda_{\text{FDM}} \mathbb{G}(X_{\text{eff}})}{\sigma_{\text{eff}}^2} + \frac{m_b \log \Lambda_{\text{soft}} \mathbb{G}(X)}{\sigma^2} \right], \quad (\text{A8})$$

$$D[(\Delta v_{\parallel}^2)] = 4\sqrt{2}\pi G^2 \rho_b \left[\frac{m_{\text{eff}} \log \Lambda_{\text{FDM}} \mathbb{G}(X_{\text{eff}})}{\sigma_{\text{eff}} X_{\text{eff}}} + \frac{m_b \log \Lambda_{\text{soft}} \mathbb{G}(X)}{\sigma X} \right], \quad (\text{A9})$$

$$D[(\Delta \mathbf{v}_{\perp})^2] = 4\sqrt{2}\pi G^2 \rho_b \left[\frac{m_{\text{eff}} \log \Lambda_{\text{FDM}} \text{erf}(X_{\text{eff}}) - \mathbb{G}(X_{\text{eff}})}{\sigma_{\text{eff}} X_{\text{eff}}} + \frac{m_b \log \Lambda_{\text{soft}} \text{erf}(X) - \mathbb{G}(X)}{\sigma X} \right], \quad (\text{A10})$$

where $\Lambda_{\text{FDM}} = 2b_{\text{max}} / (\lambda_\sigma)$, $\Lambda_{\text{soft}} = b_{\text{max}} / \varepsilon$, m_{eff} is given by equation (59), the effective velocity dispersion is $\sigma_{\text{eff}} = \sigma / \sqrt{2}$, and $X = v / \sqrt{2} \sigma$, $X_{\text{eff}} = v / \sqrt{2} \sigma_{\text{eff}} = v / \sigma$.

From the diffusion coefficients in equations (A8)–(A10), we can see that in the limit $m_b \ll m_{\text{eff}}$ ($m_b \ll m_s$, with m_s defined in eq. A1), the FDM dominates the relaxation. When $m_{\text{eff}} \ll m_b \ll m_c$, with m_c defined in equation (A2), the relaxation is dominated by the “classical” component, although the system is not a classical system since the size of the wavepackets associated with each particle is larger than the inter-particle separation, $\varepsilon \gg d$. In this regime, the wave nature of the particles affects the relaxation only through the Coulomb logarithm $\Lambda_{\text{soft}} = b_{\text{max}} / \varepsilon$. Finally, when $m_b \gg m_c$, the system is in the classical limit, and ε should be interpreted as the size of the (softened) particle.

REFERENCES

- Armengaud, E., Palanque-Delabrouille, N., Yèche, C., Marsh, D. J. E., & Baur, J. 2017, *MNRAS*, 471, 4606
- Begelman, M. C., Blandford, R. D., & Rees, M. J. 1980, *Nature*, 287, 307
- Binney, J., & Lacey, C. 1988, *MNRAS*, 230, 597
- Binney, J., & Tremaine, S. 2008, *Galactic Dynamics*, 2nd ed. (Princeton University Press)
- Cappellari, M., Scott, N., Alatalo, K., et al. 2013a, *MNRAS*, 432, 1709
- Cappellari, M., McDermid, R. M., Alatalo, K., et al. 2013b, *MNRAS*, 432, 1862
- Chandrasekhar, S. 1942, *Principles of Stellar Dynamics* (Chicago: University of Chicago Press)
- . 1943, *ApJ*, 97, 255
- Chavanis, P.-H. 2012, *Physica A*, 391, 3680
- Chavanis, P. H. 2013, *A&A*, 556, A93
- Cohen, L. 1975, in *Dynamics of Stellar Systems*, ed. A. Hayli, IAU Symposium 69 (Dordrecht: Reidel), 33
- Fouvry, J.-B., & Bar-Or, B. 2018, *MNRAS*, 481, 4566
- Hénon, M. 1960, *AnAp*, 23, 467
- Heyvaerts, J. 2010, *MNRAS*, 407, 355

- Hu, W., Barkana, R., & Gruzinov, A. 2000, *PhRvL*, 85, 1158
- Hui, L., Ostriker, J. P., Tremaine, S., & Witten, E. 2017, *PhRvD*, 95, 043541
- Iršič, V., Viel, M., Haehnelt, M. G., Bolton, J. S., & Becker, G. D. 2017, *PhRvL*, 119, 031302
- Klypin, A. A., Trujillo-Gomez, S., & Primack, J. 2011, *ApJ*, 740, 102
- Kobayashi, T., Murgia, R., De Simone, A., Iršič, V., & Viel, M. 2017, *PhRvD*, 96, 123514
- Kocsis, B., & Tremaine, S. 2015, *MNRAS*, 448, 3265
- Kormendy, J., & Ho, L. C. 2013, *ARA&A*, 51, 511
- Landau, L. 1936, *Phys. Z. Sowjetunion*, 10, 154
- Leong, K.-H., Schive, H.-Y., Zhang, U.-H., & Chiueh, T. 2018, *ArXiv e-prints*, arXiv:1810.05930
- Levkov, D. G., Panin, A. G., & Tkachev, I. I. 2018, *PhRvL*, 121, 151301
- Lin, S.-C., Schive, H.-Y., Wong, S.-K., & Chiueh, T. 2018, *PhRvD*, 97, 103523
- Lora, V., Magaña, J., Bernal, A., Sánchez-Salcedo, F. J., & Grebel, E. K. 2012, *Journal of Cosmology and Astro-Particle Physics*, 2012, 011
- Mocz, P., Lancaster, L., Fialkov, A., Becerra, F., & Chavanis, P.-H. 2018, *PhRvD*, 97, 083519
- Navarro, J. F., Frenk, C. S., & White, S. D. M. 1997, *ApJ*, 490, 493
- Nori, M., Murgia, R., Iršič, V., Baldi, M., & Viel, M. 2019, *MNRAS*, 482, 3227
- Rauch, K. P., & Tremaine, S. 1996, *NewA*, 1, 149
- Risken, H. 1989, *The Fokker-Planck Equation. Methods of Solution and Applications* (Berlin: Springer)
- Rosenbluth, M. N., MacDonald, W. M., & Judd, D. L. 1957, *PhRv*, 107, 1
- Ruffini, R., & Bonazzola, S. 1969, *PhRv*, 187, 1767
- Schive, H.-Y., Chiueh, T., & Broadhurst, T. 2014a, *Nature Physics*, 10, 496
- Schive, H.-Y., Liao, M.-H., Woo, T.-P., et al. 2014b, *PhRvL*, 113, 261302
- Tremaine, S., & Weinberg, M. D. 1984, *MNRAS*, 209, 729
- Tremaine, S. D., Ostriker, J. P., & Spitzer, L., J. 1975, *ApJ*, 196, 407
- Veltmaat, J., Niemeyer, J. C., & Schwabe, B. 2018, *PhRvD*, 98, 043509
- Viel, M., Becker, G. D., Bolton, J. S., & Haehnelt, M. G. 2013, *PhRvD*, 88, 043502
- Weinberg, D. H., Bullock, J. S., Governato, F., Kuzio de Naray, R., & Peter, A. H. G. 2015, *PNAS*, 112, 12249